



Hydrochemical evaluation of groundwater quality and human health risk assessment of trace elements in the largest mining district of South Khorasan, Eastern Iran

Ali Kazemi¹ · Milad Esmailbeigi² · Zahra Sahebi³ · Sharif Joorabian Shooshtari⁴

Received: 18 February 2022 / Accepted: 12 June 2022 / Published online: 23 June 2022
© The Author(s), under exclusive licence to Springer-Verlag GmbH Germany, part of Springer Nature 2022

Abstract

The groundwater resources of mining areas have been in a challenging condition in terms of metal pollution and human health. Therefore, this study investigated the concentration of cobalt (Co), molybdenum (Mo), selenium (Se), tin (Sn), and antimony (Sb) in groundwater samples (wells, qanats, and springs) in a heavily contaminated mining district, South Khorasan, Eastern Iran. Human health risk of the studied metals to target groups was assessed, and water quality of the studied groundwater was investigated in the study area. A total of 367 sampling sites (279 wells, 74 qanats, and 14 springs) in South Khorasan Province were selected to collect the groundwater samples from June to July 2020. Sampling was performed thrice for each sampling point, and hydrochemical parameters were evaluated using a portable multiparameter. Inductively coupled plasma mass spectrometry (ICP-MS) was used to detect the metal concentrations. Results showed an order of $Se > Mo > Sn > Co > Sb$, and hazard index (HI) demonstrated a warning condition for south of South Khorasan (drinking application), southwest of South Khorasan (Irrigation application), and east and center of South Khorasan (drinking-irrigation application). Hydrochemical parameters showed a classification of “Na + K type” and “Mixed Ca–Mg–Cl type” with an overall group of “Na–Cl–HCO₃” for sampled waters. Ficklin-Caboi diagram depicted a classification of “near-neutral low metal,” and Schoeller diagram classified studied groundwater as “good” for drinking and irrigation consumptions and “Na–Cl” type based on ion balance diagram. Based on the correlation analysis, positive relationships were recorded among EC, TDS, Cl⁻, Na⁺, sulfate, Ca²⁺, salt, total hardness, Mg²⁺, ammonia, and K⁺ measured in the water samples. In essence, arid regions of the world greatly rely upon groundwater resources for drinking and irrigation consumptions, and mining districts with a heavy load of active mines can be a serious threat to the groundwater quality and human health.

Keywords Hazard index · Mining district · Non-carcinogenic risk · Water quality · Risk assessment · South Khorasan Province

Introduction

Since 1990, a challenging stress has fetched freshwater surface resources under a harsh condition to supply healthy drinking water for human (Eman and Meško 2020). Such stressors, including precipitation shortages, environmental

Responsible Editor: Xianliang Yi.

✉ Ali Kazemi
kazemi@rocketmail.com; a-kazemi64@araku.ac.ir

Milad Esmailbeigi
milad.esmailbeigi@canberra.edu.au

Zahra Sahebi
Zahrasahebi1393@gmail.com

Sharif Joorabian Shooshtari
Joorabian@asnruk.ac.ir

¹ Department of Environmental Science and Engineering, Arak University, Arak, Iran

² Centre for Applied Water Science, Institute for Applied Ecology, University of Canberra, Canberra, ACT, Australia

³ Arvin Zist Pooya Lab, Postal Code, 1563794747 Tehran, Iran

⁴ Department of Nature Engineering, Agricultural Sciences and Natural Resources University of Khuzestan, Mollasani, Iran

pollutants, and ever-increasing water harnessing, have reinforced governments and authorities to use other alternatives such as groundwater sources (Njora and Yilmaz 2021). In arid and semi-arid regions like Iraq, Iran, Afghanistan, and Pakistan, groundwater has been a reliable reservoir to supply drinking water (Luís and Cabral 2021). In these countries, wells, qanats, and springs have been the most crucial ways to harness groundwater for both drinking and agricultural purposes (Awadh et al. 2021). Having a continuous discharge, high quality, temperature stability, and accessibility, groundwater has always been a reliable resource to supply water for drinking purposes (Siebert 2021). However, anthropogenic developments have contaminated these waters with toxic substances (Mastrocicco et al. 2021; Nivetha et al. 2021). Such destructive interferences have been occurring when at the same time the demand for clean water is increasing (Piesse 2020).

Eastern Iran has suffered from the shortage of surface water and inappropriate annual precipitation in its watersheds and mountainous areas due to the geographical position of these regions for not receiving sufficient atmospheric water (Malmal and Shiri 2021). The vast majority of these areas, including North Khorasan, Razavi Khorasan, South Khorasan, and Sistan and Baluchestan Province, occupied with deserts and lands with scattered residential areas and residence (Michel and Ghoddousi 2020). Instead, mining developments and industrial activities have extensively expanded across the Eastern Iran (Dawoudian et al. 2021). Eastern Iran is known for a diverse range of mines which are distributed in all parts of the region, and it has been challenging for the residents who have suffered from mine-polluted resources of water (Bozorgi et al. 2020). In comparison with the last 10 years, residential areas have been considerably extended and the consumption of water has increased in both agricultural and household applications (Zubaidi et al. 2020). For this, the quality and hygiene of groundwater should be an urgent priority for the government and hygienic organizations.

Groundwater has been the most crucial source of water for both drinking and agriculture purposes in Eastern Iran (Amiri et al. 2021). Qanat, known as one of the groundwater reservoirs, is one of the ancient Iranian inventions which was designed as a wondrous structure to harness water based on the gravitational forces (Talebi and Fatemi 2020). Such a great human heritage is still essential to supply water in Eastern Iran due to its merits, including being away from evaporation, no need for pumping and piping system, high quality, and stability in temperature and volume (Arefian et al. 2020). This underground aquifer extracts groundwater from the mother well and transfers water through horizontal channel to the outlet where people can use harnessed water for their

consumptions (Hein et al. 2020). Wells, in addition, are of the highly used methods for harnessing groundwater through digging deeply on the ground (Mridha and Rahman 2021). The depth of the wells depends largely on the availability of water in the underground aquifer as well as the bed rock structure (Arya et al. 2020). In terms of the groundwater variations, spring is another type of water resource in Eastern Iran although this topological system is not widely available throughout the region due to insufficient mountainous areas. The most important reason for the formation of the spring would be karst topography which allows the groundwater to travel from underground to the Earth's surface via channels caused by dissolution of soluble rocks like limestone and gypsum (Bogard et al. 2020). Therefore, well, qanat, and spring have a major contribution to water supply in Eastern Iran and the quality, quantity, accessibility, and hygiene of such groundwater are crucial for human residence.

Metal pollution has been a striking concern throughout the world, especially in developing countries which are under a serious pressure in natural resources and environment for acceleration of their development (Kumar et al. 2020; Kazemi et al. 2022a, b; Parang and Esmailbeigi 2022). Since the Industrial Revolution, human-made changes and anthropogenic activities have considerably intruded to the environment; for this, using impermissible and toxic materials, pesticides, heavy metals, farming chemicals, and mining activities has made groundwater resources at a high risk (Rajasekhar et al. 2020; Banan et al. 2022). Municipal and agricultural runoff and effluent released into the environment can firstly pollute the soil and, in turn, leach to the groundwater reducing the quality of water (Kadam et al. 2021; Shirdel et al. 2020; Behzadi Tayemeh et al. 2020). Heavy metals and metallic contaminants can be leached from the soil to the groundwater through diffusion, volatilization, erosion, oxidation, and assimilation by microorganisms, and such processes depend on the permeability, texture, and organic matter of the soil (Colombani et al. 2020). Moreover, mining activities coupling with weathering bed rock result in dissolution of trace elements and heavy metals in the groundwater which in exceeding limits could be unhealthy for consumers (Seyedi et al. 2021a, b; Çiner et al. 2021). Trace elements, including cobalt (Co), selenium (Se), tin (Sn), molybdenum (Mo), and antimony (Sb) are classified as essential elements for the human body; however, in their impermissible quantities, they can cause many health-related problems (Veisi et al. 2021; Cannas et al. 2020; Noreen et al. 2020). The literature has reported numerous studies concerning the concentration of such metals in the groundwater as well as health risk assessment (Egbueri 2020; Khalid et al. 2020; Liu and Ma 2020; Qiao et al. 2020; Zuo et al. 2020; Long et al. 2021). Heavy metals can be absorbed via ingestion, inhalation, and dermal exposures, which lead to adverse health effects, including reproductive

disorders, cancer, hypertension, gastrointestinal problems, and neurological diseases (Esmailbeigi et al. 2022; Khan et al. 2020; Yakameran et al. 2021).

South Khorasan, the study area of this research, is located in Eastern Iran (32.8653°N, 59.2164°E), which borders with North Khorasan, Semnan, Isfahan, Yazd, Kerman, and Sistan and Baluchestan Provinces (Ghorbani et al. 2021). This province has a total of 11 counties with a population of 768,898 people (2014) and a density of 5.1/km² (Bakhshi et al. 2019; Asadi et al. 2022). As people in South Khorasan rely seriously on the groundwater for drinking, irrigation, industry, and domestic animals, the quality and health status of the used water have a crucial priority in terms of peoples' health. According to the Iranian Ministry of Industries and Mines, there are more than 670 active mines in South Khorasan, which were discovered and established in all parts of the province (Shirazi et al. 2018). Chromite, dolomite, magnesite, marmorite, basalt, silicon, lead, and copper are some highly harvested mines in South Khorasan, which make the soil and bed rock of groundwater more polluted (O'Driscoll 2008). Besides, rock weathering and natural biogeochemical processes in the soil and the Earths' crust exacerbate the metal leakage and release into the groundwater resources (Esmailbeigi et al. 2021; Obasi and Akudinobi 2020). In addition, agricultural lands near groundwater aquifers in South Khorasan has caused a significant heavy metal leakage to the deepest subsoil layers due to an ever-increasing application of chemical fertilizers and pesticides (Wang et al. 2021a, b). Under these circumstances, this study intended to investigate the concentration of five trace elements (Co, Se, Mo, Sn, and Sb) as well as affective hydrochemical parameters (21 factors) in a total of 367 groundwater resources (wells, qanats, and springs) of South Khorasan. To date, there have been no comprehensive study concerning a number of groundwater samples (367 wells, qanats, and springs) in a heavily contaminated arid and mining area. Therefore, the main objectives of the present study were (i) to assess the non-carcinogenic risk of contaminated groundwater with studied metals received through oral and dermal exposure in adults and children using zoning map method, (ii) to determine the class of water in sampled stations using water specialized software, and (iii) to study the potential correlations between metal concentrations and hydrochemical parameters of groundwater resources in South Khorasan Province.

Materials and method

Study area

The study area, South Khorasan Province, is located at Eastern Iran, which lies between 32.5176° N latitude and 59.1042° E longitude and encompasses an area of about 151.

193 km² (Fig. 1A). Aquifer and groundwater are abundant in this region to supply water for a total of 11 counties consisting of a population of 768,898 people. South Khorasan is known for its unique mining resources as well as qanats as wondrous inventions relating to ancient Iranians. Having a heavy load of active mines, including iron, chromite, magnesium, copper, dolomite, marmorite, potassium, barite, and bentonite, South Khorasan has a major contribution to the gross national product of Iran (Table. 1). Groundwater is the main source of water in arid and semi-arid regions of Eastern Iran. There have been different types of groundwater in Eastern Iran, including qanat, well, and spring. Such aquifers play a pivotal role in supplying water for different consumptions like drinking and irrigation. In terms of land use of South Khorasan, the vast majority of this province is occupied with range, desert, and forest (Fig. 2B). Schematic structure of different types of groundwater resources (wells, qanats, and springs) sampled in the study area are shown in Fig. 2.

Sample collection and storage

A total of 367 sampling sites (279 wells, 74 qanats, and 14 springs) in the study area, including counties, plains, and rural areas, were selected to collect the groundwater samples from June to July 2020. The selection of sampling sites was assigned based on the population, environmental contaminants, industrial activities, and manufacturers. Sampling was performed thrice for each sampling point (1101 samples in total), and 500-ml polypropylene-labeled bottles were used to collect samples (APHA, 2012). Before sampling, bottles were carefully washed and rinsed with the water of sampling sites, and after collection, a portable multi-parameter instrument (SensoDirect 150, Lovibond, Germany) was applied to measure a range of hydrochemical factors in the field, including temperature (°C), pH, electrical conductivity (EC; mS cm⁻¹), total dissolved solids (TDS; mg L⁻¹), and dissolved oxygen (DO; mg L⁻¹). Finally, collected samples were stored in the ice box until transferring them to the refrigerator at 4.00 °C prior to starting the laboratory analysis in the lab. In the lab, total hardness (mg L⁻¹ CaCO₃), total alkalinity (mg L⁻¹ CaCO₃), bicarbonate (mg L⁻¹ CaCO₃), ammonium (N-NH₄⁺; mg L⁻¹), sulfate (So₄²⁻; mg L⁻¹), and chloride (Cl⁻ mg L⁻¹) were then measured using EDTA titrimetric, titration, titration, nesslerization, turbidimetric, argentometric methods, respectively (APHA, 2005) (Table. 2).

Sample analysis and metal concentration

Millipore filters (0.45 µm) were used to remove impurities, particles, and organic materials in the sampled waters. Few drops of HNO₃ (Merck, Germany, ultra-pure grade about

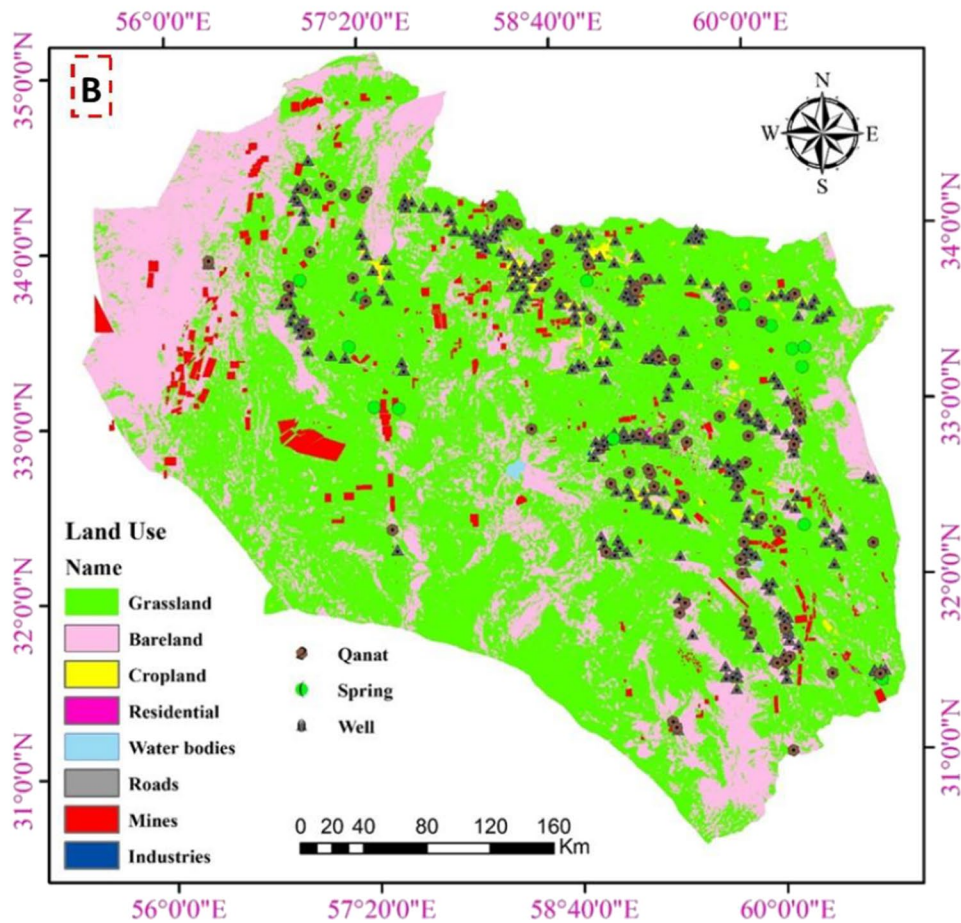
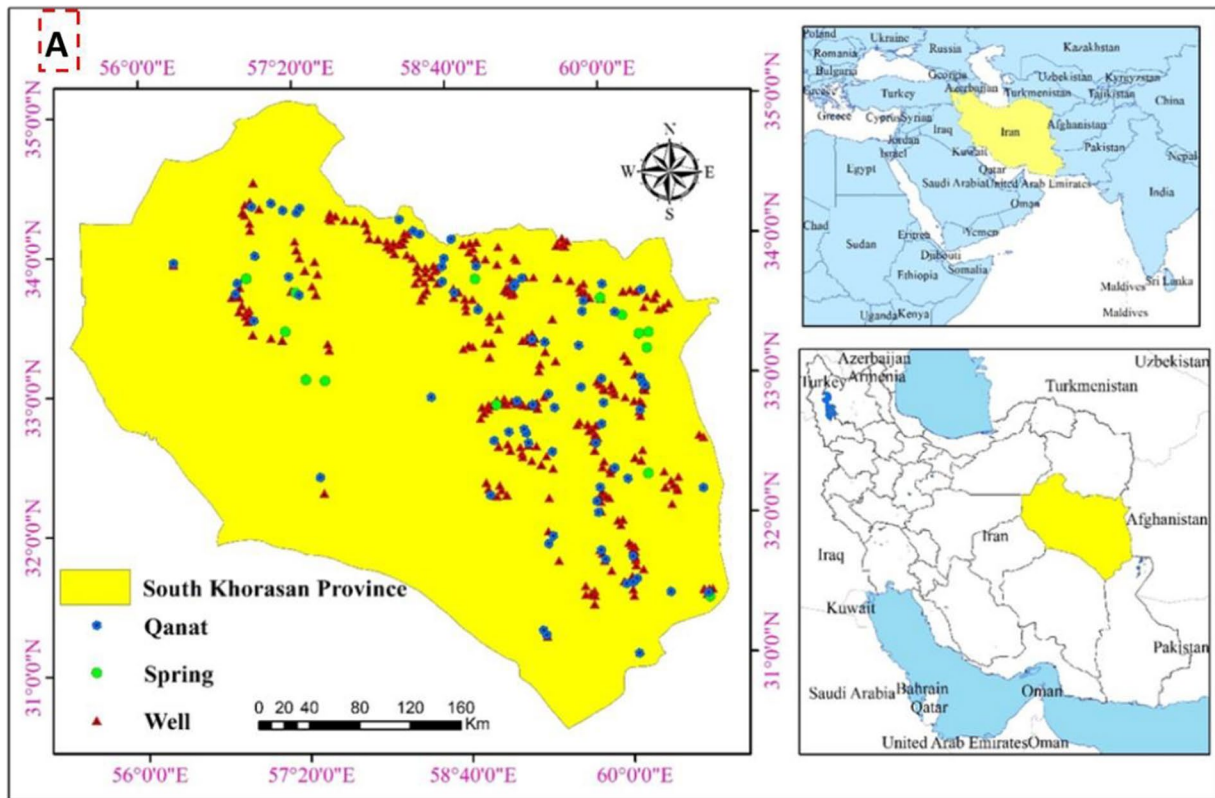


Fig. 1 Position of South Khorasan province and sampling sites for groundwater (qanat, spring, and well) on the map (A) and land use map of the study area containing studied sampling locations (B)

0.5 ml pH < 2) were then added to the samples to prevent loss of metals and bacterial and fungal growth (Tiwari and De Maio 2017). Inductively coupled plasma mass spectrometry (ICP-MS) (HP-4500 USA, equipped with auto sampler Asx-520) was used to detect the metal concentrations based on the method outlined by Zhang et al. (2008). The calibration of ICP-MS was conducted using the manufacturer’s instructions and adjusted at maximum performance and sensitivity. The polypropylene tubes were used to prepare samples for injection into the ICP-MS. All the sampling bottles and glassware cleaned by soaking in dilute acid (HNO₃ 5%) and were washed with deionized water (high purity) prior to the experiments. Prepared samples were diluted to an amount of 20 ml deionized water and then injected to the ICP-MS (Søndergaard et al. 2015). Desirable performance conditions for ICP-MS are presented in Table S1.

Quality control of measurement

For quality assurance of measured metal concentrations, limits of detection (LOD) and relative standard deviation (RSD) were examined (below 5% for all samples) using standard methods previously reported by Ilieva et al. (2018)

and Kazemi et al. (2012) (Eq. 2). LOD demonstrated a value of 1, 80, 0.5, 0.6, and 0.7 ng L⁻¹ for Co, Se, Mo, Sn, and Sb, respectively, calculated based on Eq. 1.

$$LOD = Xb1 + 3(Sb1) \tag{1}$$

where *Xb1* is the mean concentration of the blank and *Sb1* is the standard deviation of the blank.

$$RSD = 100 \times \frac{S}{|\bar{x}|} \tag{2}$$

where *S* is the sample standard deviation and $|\bar{x}|$ is the sample mean studied by analyzing the standard mixture solution in six replicates in one day and twice a day in three consecutive days, individually.

Standard limits

The concentration of studied metals and hydrochemical parameters in 367 studied sampling points (wells, qanats, and springs) were reported as mean, standard deviation, maximum, minimum, and range, and compared with standard limits released by international organizations, including the World Health Organization (WHO), United States Environmental Protection Agency (USEPA), Food and Agriculture Organization (FAO), and Iran National Standards Organization (INSO) (Table S2).

Table 1 Input values to calculate non-carcinogenic human health risk of studied metals through ingestion and dermal exposure pathways of groundwater in both adults and children

Parameter	Symbol	Unit	Exposure pathways		Reference
			Oral	Dermal	
Heavy metal concentration	C	mg L ⁻¹	-	-	-
Daily average intake	DI	L day ⁻¹	2.20	-	USEPA, 2004
Skin surface area	SA	Cm ²	-	18,000 adults, 6600 children	USEPA, 2004
Permeability coefficient	K _p	Cm/hour	-	Co: 0.0004 Se, Mo, Sn, Sb: 0.001	USEPA, 2004
Exposure time	ET	Hour/event	-	0.58 adults, 1 children	USEPA, 2004
Exposure frequency	EF	Day year ⁻¹	365.00	350.00	Mohammadi et al., 2019
Exposure duration	ED	Year	71.80	6.00	Mohammadi et al., 2019
Conversion factor	CF	L cm ⁻¹	-	0.001	USEPA, 2004
Average body weight	BW	kg	60 adults, 15 children		Mohammadi et al., 2019
Absorption factor	ABS	-	0.001		USEPA, 2004
Average time	AT	day	26,207 adults, 2190 children		Mohammadi et al., 2019
Reference dose	RfD	µg/kg/day	Co: 2.00E-02 1.60E-02 Se: 5.00E-03 6.00E-04 Mo: 2.00E-03 1.90E-03 Sn: 3.00E-04 4.00E-06 Sb: 4.00E-04 8.00E-06		

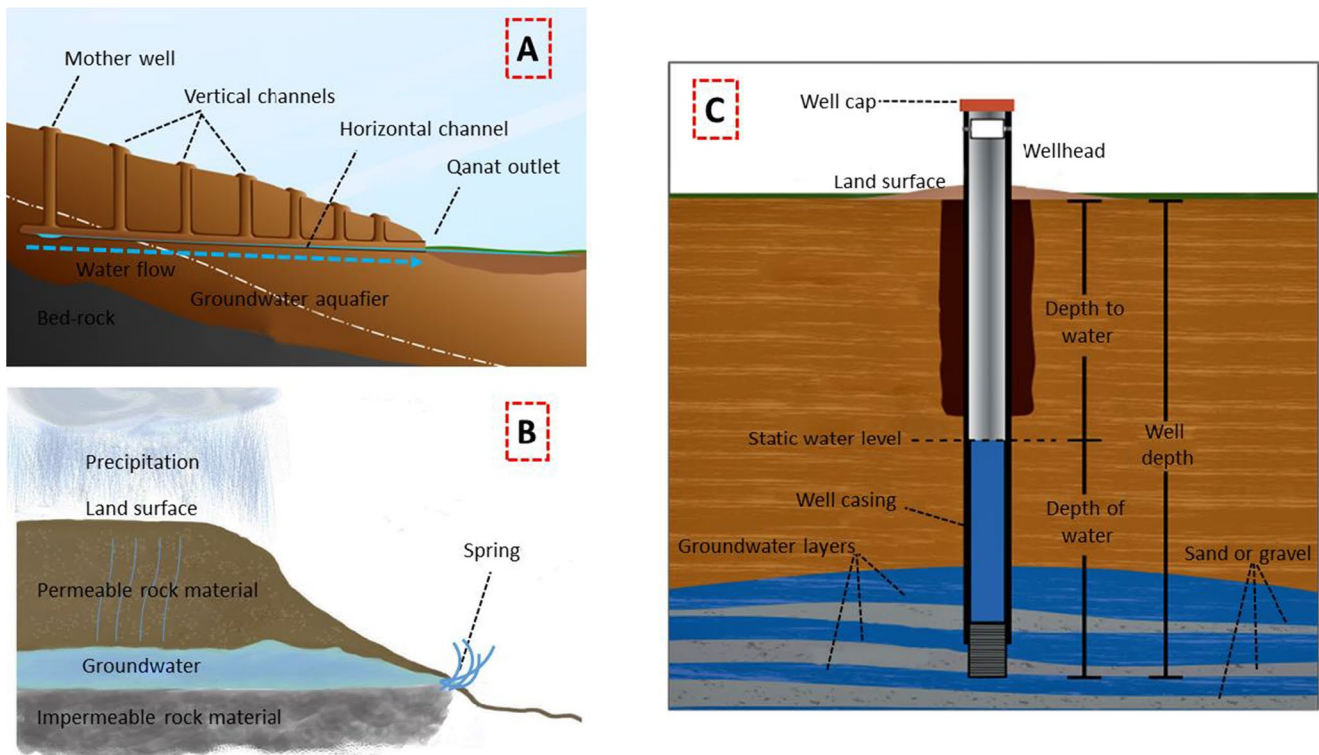


Fig. 2 Schematic structure of different types of groundwater resources in the study area (A qanat, B spring, C well)

Human health risk assessment

Non-carcinogenic health risks were measured using both dermal and oral exposure of the groundwater in the study area. For this, chronic daily intake (CDI), hazard quotient (HQ), and hazard index (HI) were considered for target people as adults and children. All the required assumptions and input values for calculations are presented in Table 1.

Chronic daily intake (CDI)

The CDI of heavy metals was calculated using Eqs. 3 and 4 for both oral (CDI_{oral}) and dermal (CDI_{dermal}) adsorption of waters to the target groups (USEPA 2004). All assumptions and input values are given in Table 1.

$$CDI_{oral} (mgkg^{-1}day^{-1}) = \frac{C_{hm} \times DI \times ABS \times EF \times ED}{BW \times AT} \quad (3)$$

$$CDI_{dermal} (mg kg^{-1}day^{-1}) = \frac{C_{hm} \times SA \times K_p \times ABS \times ET \times EF \times ED \times CF}{BW \times AT} \quad (4)$$

Hazard quotient (HQ)

HQ is defined as a ratio between CDI of heavy metal to the reference dose (R_fD) of oral and dermal adsorption. For HQ_{oral},

this ratio is between CDI_{oral} and R_fD_{oral} and was calculated using Eq. 5. HQ_{dermal} was calculated using Eq. 6 as a ratio between CDI_{dermal} and R_fD_{dermal}.

$$HQ_{oral} = \frac{CDI_{oral}}{RfD_{oral}} \quad (5)$$

$$HQ_{dermal} = \frac{CDI_{dermal}}{RfD_{dermal}} \quad (6)$$

Hazard index (HI)

The total potential non-carcinogenic health risk of heavy metals is defined as hazard index (HI) ascribed by USEPA for both oral and dermal exposures to children and adults in the study area. HI was calculated using the sum of non-carcinogenic health risk of all studied metals through oral and dermal exposure, based on Eqs. 7 and 8, respectively.

$$HI_{oral} = \sum_{i=1}^n HQ_{oral} = HQ_{Co} + HQ_{Se} + HQ_{Mo} + HQ_{Sn} + HQ_{Sb} \quad (7)$$

$$HI_{dermal} = \sum_{i=1}^n HQ_{dermal} = HQ_{Co} + HQ_{Se} + HQ_{Mo} + HQ_{Sn} + HQ_{Sb} \quad (8)$$

To categorize the HI of the studied metals to humans, a threshold value was set at 1.00, and showed that HI < 1

Table 2 Hydrochemical parameters measured in different groundwater sources in the study area

Parameter	Statistic	Well			Qanat			Spring		
		D	I	D-I	D	I	D-I	D	I	D-I
Depth (m)	Mean	107.20	94.09	131.78	16.00	32.32	32.01	-	-	-
	SD	62.29	51.22	48.82	1.41	29.52	21.95	-	-	-
Water temp (°C)	Mean	24.70	24.79	26.01	25.25	23.56	22.78	-	24.44	24.75
	SD	2.82	2.30	5.17	0.07	2.89	3.918	-	2.83	2.98
pH	Mean	7.65	7.45	7.72	7.58	7.86	7.86	-	7.33	7.88
	SD	0.28	0.26	0.28	0.35	0.38	0.36	-	0.19	0.24
EC (µS/cm)	Mean	2.42	7.13	1.60	3.48	5.02	1.11	-	8.46	0.73
	SD	1.19	3.62	0.31	4.03	2.27	0.56	-	6.32	0.38
Salt (% weight)	Mean	0.12	1.49	0.09	0.18	0.26	0.05	-	0.45	0.03
	SD	0.06	16.60	0.04	0.21	0.11	0.02	-	0.34	0.018
Total hardness (mg/l CaCO ₃)	Mean	413.20	1076.30	331.32	658.00	776.76	308.96	-	977.40	248.25
	SD	193.30	592.37	148.51	664.68	429.98	146.30	-	429.58	50.78
TDS (mg/l)	Mean	1522.99	4506.74	1032.94	2230.57	3204.7	704.7	-	5413.22	467.64
	SD	740.83	2314.70	202.62	2578.49	1441.4	354.11	-	4044.53	244.38
N-NH ₄ ⁺ (mg/l)	Mean	1.38	5.39	0.63	3.62	3.48	1.04	-	4.35	0.66
	SD	1.95	7.56	0.45	4.52	3.12	1.37	-	2.99	0.41
So ₄ ²⁻ (mg/l)	Mean	359.46	1190.23	207.10	853.54	840.70	113.95	-	1597.32	66.73
	SD	234.42	674.56	87.61	1050.19	482.01	79.04	-	1315.36	41.25
Total alkalinity(mg/l)	Mean	298.00	219.55	248.92	144.00	300.27	260.24	-	219.80	185.25
	SD	138.20	148.09	86.42	5.65	196.85	144.11	-	99.12	79.51
HCO ₃ (mg/l)	Mean	361.61	266.89	301.91	174.88	362.90	313.89	-	267.47	224.38
	SD	168.23	180.27	104.77	6.30	239.22	175.01	-	120.55	96.83
Cl ⁻ (mg/l)	Mean	449.57	1874.79	301.31	612.89	1142.0	195.56	-	1894.13	143.71
	SD	263.92	1269.14	102.23	728.27	573.47	129.15	-	1394.42	114.55
Na(mg/l)	Mean	376.66	1320.47	246.02	474.80	860.54	147.57	-	1520.30	88.94
	SD	194.63	867.12	83.66	572.20	404.44	110.16	-	1526.98	86.38
K (mg/l)	Mean	10.03	18.46	5.82	7.63	18.33	5.65	-	39.68	3.24
	SD	8.04	14.57	4.11	7.90	15.89	4.79	-	25.54	1.10
Ca (mg/l)	Mean	47.38	175.63	46.11	66.73	98.27	42.30	-	156.46	52.12
	SD	24.83	125.16	23.48	32.05	71.39	19.19	-	57.88	21.18
Mg(mg/l)	Mean	73.75	156.89	54.84	128.81	131.33	50.92	-	147.96	27.45
	SD	42.59	88.10	30.88	147.77	77.71	34.12	-	80.12	5.07

D drinking, *I* irrigation, and *DI* drinking-irrigation

means no hazardous health impacts, while $HI > 1$ displayed the possibility of non-carcinogenic health risks for people considered. Then, calculated HIs were depicted using zoning map to show the distribution of the cumulative risks of heavy metals in the study area as drinking, irrigation, and drinking-irrigation hazard index.

Hydrochemical analyses

To identify the quality, classification, and type of water in the study area, hydrochemical analyses were conducted using Piper triangular, Durov plot, Ficklin-Caboi, Schoeller, and ion balance diagram. For this, Aq.QA software (2015.1.14) was used and all hydrochemical parameters

were imported to the software for further analysis. In addition, the spatial distribution of the depth of groundwater (wells and qanats but not springs) in the study area was prepared to show the different levels of harvested water in South Khorasan.

Piper triangular diagram

To characterize the type of water in the study area, piper triangular diagram was prepared as per Piper (1944). Water samples (qanats, wells, and springs generally as groundwater) were classified based on the hydrochemical parameters and prominent ions (anions and cations) affecting the water quality. This graphical diagram included two triangular

(cations and anions) and a diamond (combination of cations and anions) showed the type of water samples using major anions (Cl , SO_4 , CO_3 , and HCO_3) and cations (Ca , Mg , Na , and K) and represented the potential chemical reactions existing in the groundwater.

Durov plot

Durov diagram (Durov, 1948) shows the possible relationships and reactions between physicochemical parameters and salinity and pH of the groundwater. This plot showed major ion milliequivalents, and dominant cations and anions are plotted by Aq.QA software in two different triangular shapes in which data values are presented on a square grid.

Ficklin-Caboi diagram

To show the possible relationships between metal concentrations and pH values, Ficklin-Caboi diagram was prepared using the method introduced firstly by Ficklin et al. (1992) and improved by Caboi et al. (1999). To do this, metal load (ML) (mg L^{-1}) was calculated as cumulative concentrations of Co , Mn , Se , Sn , and Sb , according to Eq. 9.

$$\text{ML} (\text{mg L}^{-1}) = \sum_{i=1}^n \text{metal concentrations} = C_{\text{Co}} + C_{\text{Mn}} + C_{\text{Se}} + C_{\text{Sn}} + C_{\text{Sb}} \quad (9)$$

where ML is the metal load (mg L^{-1}) and C is the concentration of each metal (mg L^{-1}).

Schoeller diagram

The water chemistry and quality can be represented via Schoeller diagram which indicates a series of anions and cations from left to the right of the diagram based on meq L^{-1} . Schoeller diagram was prepared by Aq.QA software and used SO_4 , $\text{HCO}_3 + \text{CO}_3$, and Cl as anions, and Mg , Ca , and $\text{Na} + \text{K}$ as cations to show the dominated ions contributing to the quality and classification of water for drinking and irrigation consumptions.

Ion balance diagram

Suitability of the groundwater for domestic and irrigation purposes was examined using ion balance plot to show the dominant major ions in the groundwater samples. A range of ions, including Na , Ca , Mg , SO_4 , and Cl were considered to classify the water, and the plot was prepared using by Aq.QA software.

Factor analysis

Principal component analysis (PCA) was performed to determine the major contributor hydrochemical parameters

affecting the concentration of metals as well as water quality. Variance of the factor coefficients was maximized using Varimax rotation. Eigenvalues more than 1 were considered as extracted factors, and the weights of component 1 versus components 2 and 3 were compared. Component diagram in the rotated space was prepared, and the percentage of each component in the total variance was explained (Bodrud-Doza et al. 2020).

Statistical analysis

In this study, descriptive statistics including average, minimum, maximum, standard deviation, and the range of metal concentrations in studied stations were calculated using Excel 2016 software (Windows 7; 64x). In addition, chronic daily intake (CDI), hazard quotient (HQ), and hazard index (HI) were calculated using standard formulas defined in the Microsoft Excel. To investigate the potential correlations between hydrochemical parameters, Spearman's correlation was used and applied to show possible correlations among measured factors, based on diverse colorful patterns. Principal component factor (PCA) was tested using SPSS software to extract the major contributing factor. The significance level was considered at 0.05 for all statistical analysis. Furthermore, geographical images, zoning maps, and spatial interpolation were prepared by ArcGIS (version 10.3; ESRI Inc., Redlands CA) to obtain the spatial distribution of hazard index caused by contaminated groundwater to people considered.

Results and discussion

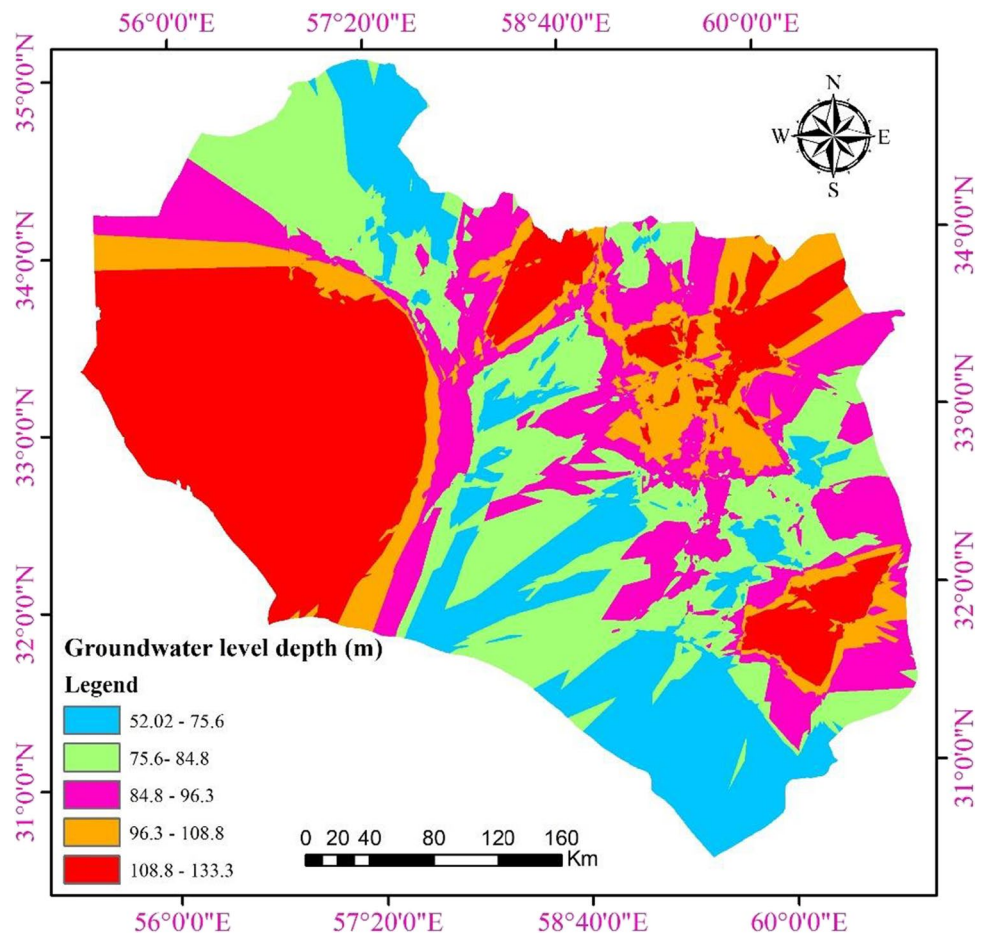
Groundwater hydrochemistry

Hydrochemical parameters measured in different groundwater resources (well, qanat, and spring) and different applications (drinking, irrigation, and drinking-irrigation) are represented in Table 2 (more details presented in supporting information, Table S3). Hydrochemical parameters, including depth (m), water temperature ($^{\circ}\text{C}$), pH, EC (mS/cm), salt (% weight), total hardness ($\text{mg L}^{-1} \text{CaCO}_3$), TDS (mg L^{-1}), N-NH_4^+ (mg L^{-1}), SO_4^{2-} (mg L^{-1}), total alkalinity (mg L^{-1}), HCO_3 (mg L^{-1}), Cl^- (mg L^{-1}), Na (mg L^{-1}), K (mg L^{-1}), Ca (mg L^{-1}), and Mg (mg L^{-1}), were measured and reported as mean, minimum, maximum, standard deviation, and range (Table. 2). Based on the findings, pH values showed a range of 6.87 to 8.90 with a mean value of 7.64 and represented the strength of the water to react with acidic and alkaline metals included. EC has been considered as one of the leading hydrochemical parameters in determining the quality of water, and, in this study, results showed a range of 0.26 to 20.90 mS/cm for groundwater in different

applications in the study area (Table. 2). Such values for EC were agreed with the permissible limits released by WHO (2011) and Institute of Standards & Industrial Research of Iran (ISIRI). Total dissolved solid (TDS) directly influences the quality of water for drinking and irrigation purposes. In this research, TDS values ranged from 169.44 to 13,363.61 mg L⁻¹ throughout all sampled groundwater resources. Na and Cl concentrations represented a range of 12.59 to 284.23 and 25.66 to 7592.95 mg L⁻¹, respectively. Na⁺ and Cl⁻ play a crucial role in ion content and balance of the groundwater quality and act as major contributors and dominating ions in the constitution of TDS. Indeed, Na⁺ and Cl⁻ are the dominating cations, and these are directly proportional to TDS. This means that changes in the concentration of Na⁺ and Cl⁻ can directly influence the TDS, and in turn, salinity of groundwater (Saxena et al. 2003). In addition, spatial distribution of groundwater depth (wells and qanats), showing different harvested levels of water in the study area, is depicted in Fig. 3. Based on the findings, the deepest groundwater resources with a depth from 108.80 to 133.30 m were in the west and east regions of the South Khorasan, representing the massive water extraction in these parts of the study area. This is because

in east and west areas of South Khorasan, the groundwater aquifers located in the deepest part of the ground due to the shortage and/or lack of discharging surface waters into the underground reservoirs. In contrast, wells and qanats levels with a depth from 52.02 to 84.80 m were distributed mostly in the south, center, and north of the study area where the underground reservoir situated in the lower levels of the land. Wu et al. (2020) reported that the greatest concentration of arsenic detected in higher depth (> 100) as they claimed the deeper wells at 41–90 m and above 90.00 m showed As mean concentrations of 51 and 123 µg L⁻¹, respectively. Detected metal concentrations and hydro-chemical parameters were compared with the international and national standards (WHO, 2011; USEPA 2012; FAO, 1985; and INSO 1997). According to the standards, TDS in studied locations showed a mean value of 3419.40 mg L⁻¹, whereas Iran, WHO, and USEPA reported 1000.00, 600.00, and 500.00 mg L⁻¹ for drinking purposes (Sig < 0.05), respectively. In addition, Na⁺ and Cl⁻ ions had mean values of 975.16 and 1359.58 mg L⁻¹ compared with the Iran, WHO, and USEPA standards at 200.00, 50.00, and 20.00 (Na⁺) and 250.00, 200.00, and 250.00 (Cl⁻) (Sig < 0.05). Se concentrations did reveal a mean value of 140.24 mg L⁻¹

Fig. 3 Spatial distribution of groundwater depth (wells and qanats) in the study area



compared to Iran, WHO, and USEPA standards at 10.00, 40.00, and 50.00 (Sig < 0.05), respectively. In addition, SO₄²⁻ concentrations exceeded the Iran, WHO, and USEPA standards (250.00 mg L⁻¹) at 889.04 mg L⁻¹ (Sig < 0.05). In line with our results, Jha et al. (2020) conducted a study to assess the quality of groundwater for drinking consumptions, and hydrochemical parameters showed exceeding and permissible values for (TDS, Na⁺, Cl⁻, K⁺, F⁻, and Hardness) and (Ca²⁺, Mg²⁺, and SO₄²⁻) ions compared with WHO limits for studied groundwater samples. The impacts of mining activities on the hydrochemical parameters of groundwater connected mainly to complex physical–chemical reactions, including weathering, dissolution, and oxidation. Such reactions alongside the leaching and erosion due to groundwater and surface runoff, causing acid mine drainage (AMD) with high contents of sulfate and heavy metals. AMD directly influence the geochemical attributes of soil and bed rock, and in turn, leads to heavy metal pollution and the deterioration of groundwater soils in mining areas. Acidic material originating from mines can increase the solubility of various salts, change the pH, TDS, alkalinity, EC, and HCO₃⁻ (Peng et al. 2015).

Trace element concentration

The concentrations of studied metals, including Co, Se, Mo, Sn, and Sb (µg L⁻¹) in different groundwater resources (i.e., well, qanat, and spring) and different applications (drinking, irrigation, and drinking-irrigation), are displayed in Table 3 as per mean, minimum, maximum, standard deviation, and range. The mean concentrations of Co were 0.23 ± 0.57, 7.00 ± 14.57, and 0.77 ± 1.42 µg L⁻¹ for wells with drinking, irrigation, and drinking-irrigation applications, respectively. In sampled qanats, Co concentrations showed 3.11 ± 4.52, 4.05 ± 7.62, and 0.60 ± 68.71 µg L⁻¹ drinking, irrigation, and drinking-irrigation consumptions, respectively. In studied springs, Se concentrations showed 9.82 ± 15.63 and 3.66 ± 7.97 µg L⁻¹ in drinking and drinking-irrigation purposes, respectively. Ravanipour et al. (2021) investigated the concentrations of Se, Co, and Mo at 42.68 ± 21.23, 22.76 ± 42.65, and 18.92 ± 14.11 µg L⁻¹, respectively. In the present study, in drinking, irrigation and both, Se concentrations showed a range of 51.34 ± 61.87, 107.35 ± 181.93, and 50.64 ± 66.48 µg L⁻¹ (in wells); 51.85 ± 52.82, 117.62 ± 150.00, and 66.19 ± 10.11 µg L⁻¹

Table 3 Metal concentrations (µg L⁻¹) in different groundwater resources in the study area

Metal	Statistic	Well			Qanat			Spring		
		D	I	D-I	D	I	D-I	D	I	D-I
Co	Mean	0.23	7.00	0.77	3.11	4.05	0.60	-	9.82	3.66
	Min	0.00	0.00	0.00	0.00	0.00	0.00	-	1.14	0.00
	Max	2.78	125.50	7.23	6.31	46.94	6.53	-	37.72	23.18
	SD	0.57	14.75	1.42	4.52	7.62	68.71	-	15.63	7.97
	Range	2.78	125.50	7.23	6.31	46.94	6.53	-	36.57	23.18
Se	Mean	51.34	107.35	50.64	51.85	117.62	66.19	-	44.58	73.42
	Min	0.00	0.00	1.68	14.50	0.00	7.17	-	4.42	1.36
	Max	283.50	1615.00	299.70	89.20	934.30	272.90	-	140.90	229.30
	SD	61.87	181.93	66.48	52.82	150.00	10.11	-	55.55	82.23
	Range	283.50	1615.00	298.13	74.70	934.30	265.73	-	136.47	227.93
Mo	Mean	11.10	22.11	19.07	8.86	21.55	11.23	-	19.14	10.29
	Min	3.57	0.74	0.00	8.63	2.22	0.23	-	5.96	2.72
	Max	27.99	208.90	130.60	9.10	137.80	43.64	-	43.12	25.94
	SD	6.60	29.08	28.38	0.23	23.34	10.11	-	16.15	9.35
	Range	24.41	208.1	130.6	8.86	135.57	43.40	-	37.15	23.21
Sn	Mean	0.77	29.26	2.63	0.21	1.50	2.97	-	6.59	0.43
	Min	0.00	0.00	0.00	0.00	0.00	0.00	-	0.6557	0.00
	Max	3.93	6034.00	62.32	0.43	15.23	73.12	-	28.91	1.03
	SD	0.92	407.68	10.60	0.35	3.19	13.51	-	12.47	0.39
	Range	3.93	6034.00	62.32	0.43	15.23	73.12	-	28.25	1.03
Sb	Mean	0.48	0.61	0.40	0.29	0.61	0.74	-	0.70	0.47
	Min	0.00	0.00	0.00	0.00	0.00	0.00	-	0.58	0.00
	Max	1.21	20.39	0.73	0.59	3.72	10.63	-	0.89	0.83
	SD	0.31	1.47	0.27	0.42	0.59	1.92	-	0.15	0.30
	Range	1.21	20.39	0.73	0.59	3.72	10.63	-	0.31	0.83

D drinking, I irrigation, and DI drinking-irrigation

(in qanats); and –, 44.58 ± 55.55 , and $73.42 \pm 82.23 \mu\text{g L}^{-1}$ (in springs). Our findings showed that metal concentrations were in a decreasing order as $\text{Se} > \text{Mo} > \text{Sn} > \text{Co} > \text{Sb}$, and qanats with the irrigation usages had the highest Se values at $117.62 \pm 150.00 \mu\text{g L}^{-1}$. It is highly possible that in qanats groundwater experiences a long-distance flow (from 500 m to more than 100 km) with a relatively slow current underground, and therefore, metals have enough time to be resolve in the water (Kazemi et al 2022a, b). In addition, Sb demonstrated concentrations below 1.00 in all sampled wells, qanats, and springs with different applications considered. Sayadi et al. (2020) stated that the concentration of Cd and Cr in sampled qanats in eastern Iran was at 0.02 and $1.09 \mu\text{g L}^{-1}$, respectively. As concentrations showed high values for groundwater resources in 12% of the studied population in rural areas, and geochemical reactions, topography, soil chemistry were considered as most reasons for metal presence in the groundwater (Bindal and Singh 2019). In a similar study, Cui et al. (2021) studied the ecological, health risk assessments, and water quality of heavy metals in the Haihe River, China. They stated that Sb concentrations posed health risks to human, but Co and Sn showed ecological risk to the environment. In addition, their sensitivity analysis results showed Co, Sn, and Sb were between the major contributing parameters in water, as well as Se in the fish body in the study area. In this study, in drinking, irrigation, and both, results demonstrated that Mo concentrations ranged from 11.10 ± 6.60 , 22.11 ± 29.08 , and $19.07 \pm 28.38 \mu\text{g L}^{-1}$ (in wells); 8.86 ± 0.23 , 21.55 ± 23.34 , and $11.23 \pm 10.11 \mu\text{g L}^{-1}$ (in qanats); and –, 19.14 ± 16.15 , and $10.29 \pm 9.35 \mu\text{g L}^{-1}$ (in springs). In a study, Tsai et al. (2016) reported Mo concentrations in groundwater of potentially and non-potentially contaminated areas in Taiwan at 0.0058 mg L^{-1} and 0.0022 mg L^{-1} , respectively. Such findings were lower than what we discovered in South Khorasan. The World Health Organization recommended 0.07 mg L^{-1} for Mo in drinking water for human that their values were below this suggested value. In the south of South Khorasan, there are many active mines and miners harvest materials associated with Mo in their products such as molybdenum mines. Wang et al. (2021a, b) used a water quality criteria for water quality standard in China and assessed the toxicity of 15 metals and metalloids based on the exposure factors in water and fish species. Findings revealed that Cd, Cu, Zn, As, Hg, and Mn have potential long-term health risk ($\text{HQ} \geq 1$) to the local population of the study area. However, Sb, Se, Co, Pb, and Sn showed no risk to target human groups. Sn values revealed 0.77 ± 0.92 , 29.26 ± 407.68 , and $2.63 \pm 10.60 \mu\text{g L}^{-1}$ (in wells); 0.21 ± 0.35 , 1.50 ± 3.19 , and $2.97 \pm 13.51 \mu\text{g L}^{-1}$ (in qanats); and –, 6.59 ± 12.47 , and $0.43 \pm 0.39 \mu\text{g L}^{-1}$ (in springs). Tin is one of the not-well-studied or unstudied toxic metals in mining areas of the world. In South Khorasan, there are not many mines

harvesting the tin, but some miners discover this metal in other mines. Alshaebi et al. (2009) studied the concentration and contamination of heavy metals in an abandoned tin mine in Malaysia. The results suggested that there is a vital increase of heavy metal risk in this area. The type and number of mines in the study area are reported in Table 4. A diverse range of mines, including magnesite, granite, gips, chromite, wollastonite, silicon, marmorite, garnet, fluorine, dolomite, iron, Chinese, stone, copper, gold, bentonite, travertine, bauxite, maren, barite, potassium, calcite, lead, hematite, kaolinite, perlite, CaCO_3 , and coal were considered in a total of 11 counties in South Khorasan. South Khorasan is known as a mining city possessing a number of active and abandoned mines. Obasi and Akudinobi (2020) reported that in the areas with heavy load of mining activities, the concentration of carcinogenic metals, including Pb, As, Hg, Se, and Cd, was greater than the other regions due to the mineralization processes. In the mining communities, mining developments can adversely affect the soil and cause contamination of surface and groundwater. In our study, it is obvious that different types of mines have been distributed across the study area where mine wastes compose acid mine drainage and sulfide leading to heavy metal contamination in the soil and groundwater. Literature reported that copper mines near Kilembe, Western Uganda, have polluted River Nyam-wamba which is close to the mining sites (Abraham and Susan 2017). There is a soil–water interaction through weathering of the mineral deposits, especially in the areas with pore soils. The present study included a total of 11 counties with a number of rural areas located in close to active and abandoned mines. Tabas in the west and Birjand in the center of South Khorasan had the largest and lowest number and type of mining cites, respectively (Table. 1).

Health risk assessment

As the health effects of studied metals are classified as non-carcinogenic elements, chronic daily intake (CDI) and hazard quotient (HQ) calculated for adults and children who received studied metals through oral and dermal exposures (Table 5). In addition, hazard index (HI) showing the total potential non-carcinogenic risks of studied metals for adults is presented in Table 6. CDI, HQ, and HI were calculated for children as a vulnerable group residing in South Khorasan (Tables 7 and 8). Furthermore, spatial distribution of HI (potential non-carcinogenic risks) is shown in Figs. 4, 5, and 6 for drinking, irrigation, and drinking-irrigation applications, respectively. According to the results, southern parts of the study area did show the greatest HI for both studied groups (adults and children), who used groundwater for drinking consumptions, exposed to metals through oral and dermal exposures (Fig. 4). $\text{Se} > \text{Mo} > \text{Sn} > \text{Co} > \text{Sb}$. Se in trace quantities is essential for the nutrition of

Table 4 The type of mines in the study area (based on the separate counties)

Mine	Boshrooyeh	Birjand	Khosf	Darmiyān	Zirkoh	Sarayan	Sarbisheh	Tabas	Ferdos	Ghaen	Nehbandan
Magnesite	-	-	*	*	*	-	*	*	-	-	*
Granit	*	*	*	*	-	-	*	-	-	-	*
Gips	-	-	-	*	-	*	-	*	*	*	*
Chromite	*	-	-	*	*	-	*	-	-	-	*
Wollastonite	-	-	-	-	-	-	-	-	-	-	*
Silicon	-	*	-	-	-	-	-	*	*	-	*
Marmorite	*	-	*	*	-	-	*	*	*	*	-
Garnet	-	*	-	-	*	-	-	-	-	-	*
Fluorine	-	-	-	-	-	-	-	*	-	-	*
Dolomite	*	-	*	-	-	-	-	*	*	-	*
Iron	*	-	-	-	*	-	-	*	-	*	*
Chinese stone	*	-	-	-	-	-	-	-	-	-	*
Copper	-	-	*	*	*	-	*	*	*	*	*
Gold	*	-	*	-	-	-	-	-	-	-	*
Bentonite	*	*	*	*	-	*	-	*	*	*	*
Travertine	-	-	-	*	-	-	*	*	-	*	-
Bauxite	-	-	-	-	*	-	-	*	-	*	-
Maren	-	-	-	*	-	*	-	-	-	*	-
Barite	*	-	-	-	-	-	-	*	*	-	*
Potassium	-	-	-	-	-	-	-	*	-	-	-
Calcite	*	-	-	-	*	-	-	*	-	-	-
Lead	*	-	-	-	-	*	-	-	-	-	-
Hematite	*	-	-	-	*	-	-	*	-	-	-
Kaolinite	*	-	-	*	-	*	-	*	*	-	-
Perlite	-	-	-	-	*	-	*	-	*	-	-
CaCO ₃	-	*	*	*	*	*	-	-	-	*	-
Coal	-	-	*	-	*	*	*	*	-	-	-

(*) indicates inclusion and (–) shows exclusion on the mines

human body 0.2 mg day⁻¹), but exceeding concentrations (0.7–7.00 mg day⁻¹) lead to destructive changes in the hair and fingernail, peripheral nervous system, liver and brain health, fatigue, and irritability (WHO 2011). Unacceptable

values for Mo showed various hazards to the human health, especially those who live in heavily mining areas where people greatly rely upon groundwater resources. Toxic values of Mo can interfere in the digestion system function and leads

Table 5 Chronic daily intake (CDI) and hazard quotient (HQ) in oral and dermal exposure pathways in different applications for adults (mean values)

Source	Index	Metal				
		Co	Se	Mo	Sn	Sb
Drinking	CDI _{oral}	2.66241E-08	1.96685E-06	3.85445E-07	2.46656E-08	1.71491E-08
	CDI _{dermal}	7.40634E-11	1.36785E-08	2.65321E-09	1.71538E-10	1.19264E-10
	HQ _{oral}	4.62896E-08	2.27976E-05	1.39643E-06	4.28845E-05	1.4908E-05
Irrigation	HQ _{dermal}	2.42194E-07	3.9491E-06	8.0466E-07	7.31682E-08	2.24168E-08
	CDI _{dermal}	6.7374E-10	2.74642E-08	5.59604E-09	5.08851E-10	1.55898E-10
	HQ _{oral}	1.21097E-05	0.000789819	0.00040233	0.000243894	5.60419E-05
Drinking-irrigation	HQ _{dermal}	4.21088E-07	4.57736E-05	2.94529E-06	0.000127213	1.94873E-05
	CDI _{oral}	3.71755E-08	2.19269E-06	5.4254E-07	9.15215E-08	2.02778E-08
	CDI _{dermal}	1.03416E-10	1.52491E-08	3.77312E-09	6.36491E-10	1.41023E-10
	HQ _{oral}	1.86E-06	43.85E-05	27.10E-05	30.50E-05	5.06946E-05
	HQ _{dermal}	6.46E-08	2.54152E-05	1.98585E-06	0.000159123	1.76279E-05

Table 6 The total potential non-carcinogenic health risks (HI) in both oral and dermal exposure pathways for adults

Source	Statistics	HI _{oral}	HI _{dermal}
Drinking	Mean	7.13E-04	8.20E-05
	Min	2.37E-04	7.38E-06
	Max	2.52E-03	3.36E-04
Irrigation	Mean	1.50E-03	1.95E-04
	Min	2.81E-06	9.76E-08
	Max	1.60E-02	5.76E-03
Drinking-irrigation	Mean	10.00E-03	20.00E-06
	Min	1.59E-04	4.08E-06
	Max	1.19E-02	50.00E-04

to histopathological lesions in the liver and kidney tissues (Kuiper et al. 2015).

In contrast, northern areas of south Khorasan had the lowest hazard index for adults and children. To support this, Nehbandan (south of South Khorasan) is one of the most mining cities in South Khorasan with 15 different types of mines and wells and qanats with an average depth of 52.02–75.60 m. Literature has reported that the distribution and abundance of mining sites play a leading role in the soil and groundwater contamination (Obasi and Akudinobi 2020). Moreover, it is claimed that the depth of groundwater can significantly affect the pollution status of water when the aquifer is in close interactions with surface contaminants because of mineralization process (Krogulec and Malecki 2020); therefore, it is highly possible that in southern areas, the non-carcinogenic risk of studied metals is in a cautious condition for both adults and children. Results of this study demonstrated that north counties of South Khorasan did undergo the lowest hazards for investigated human groups. The frequency of mining sites showed that Ferdous, Ghaen, Boshrooyeh, Zirkoh, Sarayan, and Birjand in the north of

South Khorasan had different active mines and the depth of harvested groundwater was as greater as the respective southern sampling points. Findings concerning the spatial distribution of HI values for adults and children in irrigation applications are presented in Fig. 5. It is clear that the west areas did show the lowest HI for consumers through oral and dermal exposure. To support this, Tabas (west of South Khorasan) is the largest county in the study area and contains a vast area of desert and bare lands without agricultural activities as shown in the land-use map (Fig. 1A). Khosf and Nehbandan in the north and Ferdous and Boshrooyeh in the south of the study area demonstrated the highest HI for water consumers through oral exposure (Fig. 5a and b). Such areas have the largest percentage of agricultural activities as well as mining developments. Oral exposure is the main pathway for human exposure to the metal contaminants, and the ingestion system can be destructed via toxic metal exposure. Dermal exposure of HI showed a dangerous condition for irrigation applications in Khosf and Tabas (south-west of South Khorasan) (Fig. 5c and d). Phan et al. (2020) reported that the vast majority of sampled groundwaters

Table 8 The total potential non-carcinogenic health risks (HI) in both oral and dermal exposure pathways for children

Source	Statistics	HI _{oral}	HI _{dermal}
Drinking	Mean	27.66E-04	33.39E-05
	Min	5.10E-06	1.61E-07
	Max	29.17E-03	95.36E-04
Irrigation	Mean	15.04E-04	19.58E-05
	Min	2.81E-06	9.76E-08
	Max	16.04E-03	57.63E-04
Drinking-irrigation	Mean	19.40E-04	13.52E-05
	Min	28.89E-05	2.72E-06
	Max	21.79E-03	33.62E-04

Table 7 Chronic daily intake (CDI) and hazard quotient (HQ) in oral and dermal exposure pathways in different applications for children

Source	Index	Metal				
		Co	Se	Mo	Sn	Sb
Drinking	CDI _{oral}	4.84074E-08	3.57609E-06	6.93649E-07	4.48465E-08	3.11802E-08
	CDI _{dermal}	1.22544E-10	2.26322E-08	4.38995E-09	2.83823E-10	1.97332E-10
	HQ _{oral}	2.42037E-06	0.000715218	0.000346825	0.000149488	7.79505E-05
	HQ _{dermal}	7.65899E-08	3.77204E-05	2.3105E-06	7.09558E-05	2.46665E-05
Irrigation	CDI _{oral}	4.40353E-07	7.18017E-06	1.46302E-06	1.33033E-07	5.32421E-08
	CDI _{dermal}	1.11476E-09	4.54416E-08	9.2591E-09	8.41935E-10	3.36957E-10
	HQ _{oral}	2.20176E-05	0.001436035	0.000731509	0.000443444	0.000133105
	HQ _{dermal}	6.96723E-07	7.57361E-05	4.87321E-06	0.000210484	4.21196E-05
Drinking-irrigation	CDI _{oral}	6.75919E-08	3.9867E-06	9.86437E-07	1.66403E-07	3.68688E-08
	CDI _{dermal}	1.71109E-10	1.00924E-08	2.49717E-09	4.2125E-10	9.33336E-11
	HQ _{oral}	3.37959E-06	0.00079734	0.000493219	0.000554676	9.2172E-05
	HQ _{dermal}	1.06943E-07	1.68206E-05	1.3143E-06	0.000105312	1.16667E-05

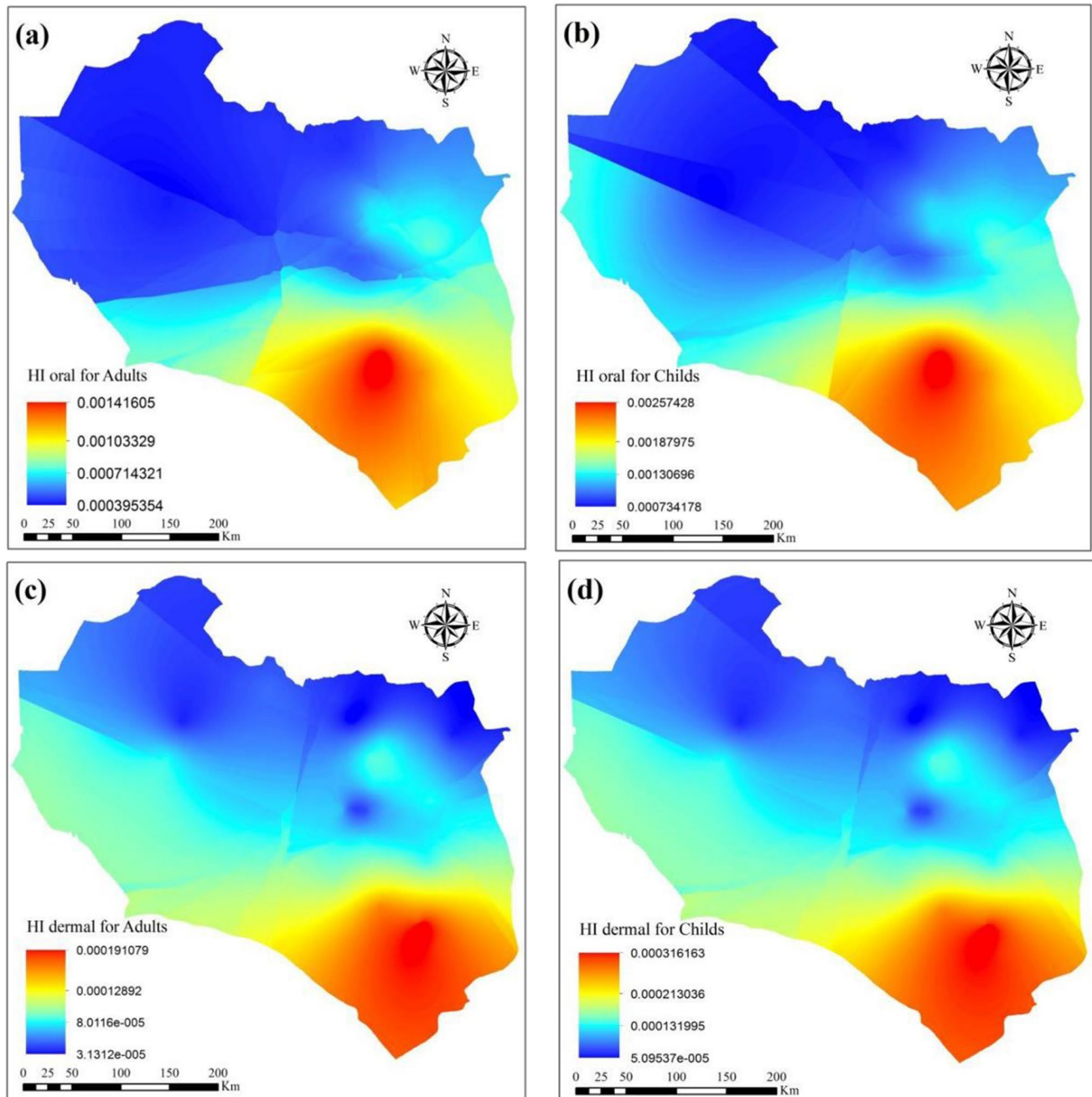


Fig. 4 Spatial distribution of hazard index (potential non-carcinogenic risks) of the groundwater used for drinking purposes in the study area (**a** oral exposure for adults; **b** oral exposure for children; **c** dermal exposure for adults; **d** dermal exposure for children)

revealed non-carcinogenic risks for water consumers. In the present study, groundwater stations used for mixed applications of drinking and irrigation showed a cautious condition for water consumers lived in Dermian (in the east), Birjand (in the center), and Khosf (in the south) in both oral and dermal exposure. However, northern and western locations had the lowest HI values (Fig. 6). Shams et al. (2020) investigated the carcinogenic and non-carcinogenic health risks of trace metals in the groundwater around mines in Joghatai,

Iran. They reported that the concentration of chromium was higher than the respective international limits, which leads to increasing the chance of cancer in the body. Hazard index for chromium was greater for children than adults. In another supportive study, non-carcinogenic human health risk of heavy metals in the groundwater of Torbat Heydariyeh, southeastern of Iran, was investigated. Results revealed that infant, children, teenagers, and adults of the exposed population were the most vulnerable groups to Pb, Cd, and

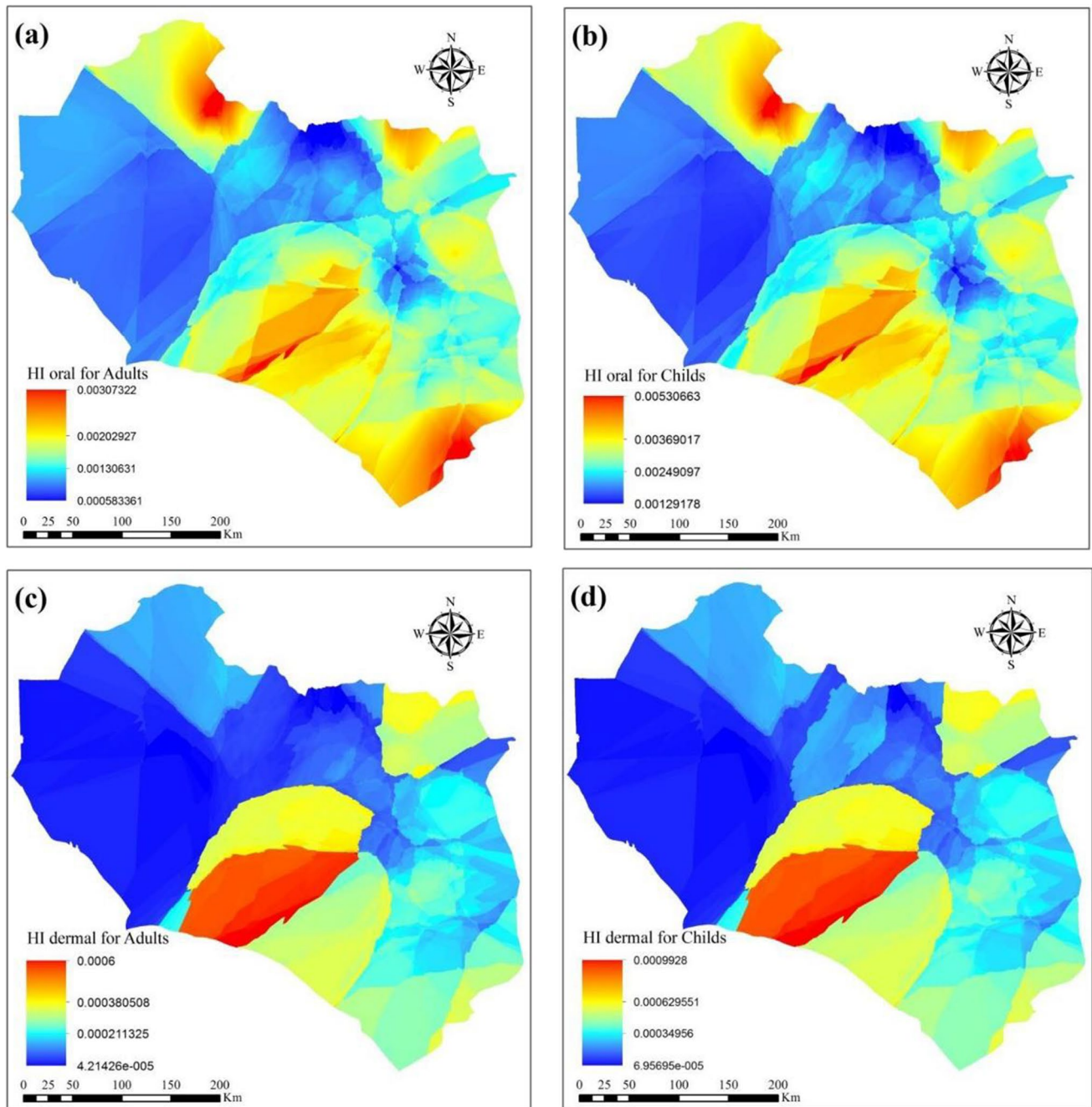


Fig. 5 Spatial distribution of hazard index (potential non-carcinogenic risks) of the groundwater used for irrigation purposes in the study area (**a** oral exposure for adults; **b** oral exposure for children; **c** dermal exposure for adults; **d** dermal exposure for children)

Cr as carcinogenic metals in the groundwater of this region (Soleimani et al. 2020). There are three ways for human exposure to heavy metals, including oral (ingestion), dermal, and inhalation. For water consumers, oral and dermal exposures are the main route of the trace metals to enter into the body through drinking and washing the body surface (Khan et al. 2020; Yakameran et al. 2021). In our previous study, we showed that the non-carcinogenic and carcinogenic risks

of Cr_T in qanat waters are in a cautious level for those consumers in the south of South Khorasan as this area is heavily polluted with mining activities (Kazemi et al. 2022a, b). As mentioned in Tables 6 and 8, HI values for adults showed lower values ($7.13E-04$) compared to children ($27.66E-04$) via oral exposure route in drinking purposes. In irrigation and irrigation-drinking purposes, adults showed the highest HI values compared to children. Through dermal exposure,

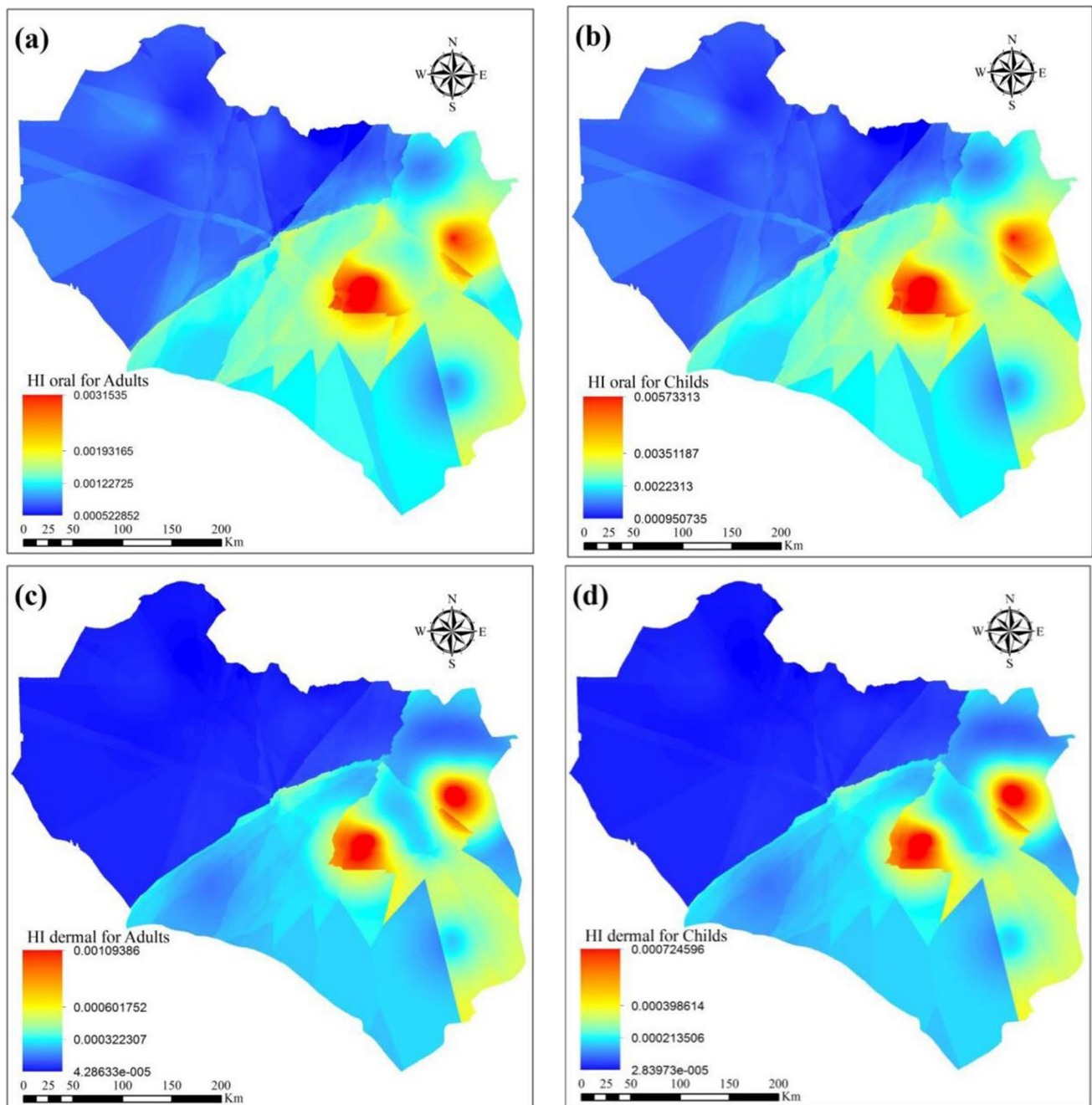


Fig. 6 Spatial distribution of hazard index (potential non-carcinogenic risks) of the groundwater used for drinking-irrigation purposes in the study area (**a** oral exposure for adults; **b** oral exposure for children; **c** dermal exposure for adults; **d** dermal exposure for children)

HI demonstrated largest values for children at $33.39\text{E-}05$ compared to adults with a value of $8.20\text{E-}05$ in drinking purposes. In oral exposure, in addition, children had lower HI at $19.58\text{E-}05$ compared to adults with $1.95\text{E-}04$. In dual purpose sources (irrigation-drinking), children did show more HI at $13.52\text{E-}05$, while adults had $20.00\text{E-}06$. There are many factors influencing the risk of contaminants to the health of human body, and uncertainty in the risk assessment

analyses is an undeniable fact. Although it is true that calculations in the health risk analyses can give us a viable understanding in terms of the potential hazards for humans, many factors such as gender, age, food habitat, level of health, possible stressors, pregnancy, smoking, and knowledge could also impact risk assessment decisions. This means that it is hard to say that an element has non-carcinogenic effects to a specific target group only based on the calculated

information. For instance, the level of knowledge among people in our study area is not very acceptable and they do not know the hazards of toxic materials to their health. EPA (2004) stated that uncertainties are part of almost all risk assessments and the effects of chemicals at different life stages and different comorbidities, the effects of exposures to complex mixtures, and the effects of chemicals are the most important uncertainties in ecotoxicological studies.

Hydrochemistry analyses

Piper triangular diagram

The water quality and classification of the groundwater in the study area have been displayed using piper triangular diagram (Fig. 7A). Cation triangular showed that 60% of studied groundwater relates to “Na + K type” and 40% of the samples classified as “mixed type” in the study area. In terms of anion triangle, 55% of groundwater samples categorized in “Cl type,” 25% were in “HCO₃ type,” and the rest of the samples were grouped as “mixed type.” In addition, as diamond diagram showed, 50% of groundwater was classified as “Na-Cl” type and the rest of the samples were in “mixed Ca–Mg–Cl type.” Overall, piper triangular diagram showed that the water samples were predominantly affected by Na, Cl, and HCO₃ ions and represented a “Na-Cl-HCO₃” type for the groundwater considered. Zakir et al. (2020) used piper triangular diagram to classify surface and groundwater of Jamalpur Sadar area, Bangladesh. They stated that, in terms of cations, 60% and 59% of sampled locations were in “Ca type” for groundwater and surface water, respectively, while for anions water samples were in “HCO₃ type” at 100 and 86% for groundwater and surface water, respectively. The composition of hydrochemical parameters plays a crucial role in determination of water classification and the dominance of anions and cations is important to show the predominance of ions in the groundwater (Ravikumar et al. 2015). In the present study, hydrofacies diagram showed that alkalis (Na⁺ and K⁺) exceeded the alkaline earths (Ca²⁺ and Mg²⁺) while acids of (Cl⁻ and HCO₃⁻) were dominant on acids of (SO₄²⁻ and CO₃²⁻). Such findings were line with those reported by Umamageswari et al. (2019) who investigated the hydrochemical processes in the groundwater environment of Batlagundu block, Dindigul district, Tamil Nadu. To support this, Vasilache et al. (2020) claimed that the chemical structure of the aquifer has a major role in the indication of water type because of ion-exchange and other possible reactions, including evaporation, dissolution, and salination underground. For the evaporation, precipitation of carbonate minerals at high salinity due to evaporation reduces Ca activity in the groundwater, which triggered the solubility of gypsum and fluorite through common ion effect. In addition, mineral dissolution in groundwater comes

from interaction with the geologic materials in flow through depending on the speed, volume, and chemical structure of rock bed (Rajmohan et al. 2021). Mohamed (2019) outlined a Ca-CO₃ type for groundwater samples as cations and anions represented an order of Ca²⁺ > Na⁺ > Mg²⁺ > K⁺ and HCO₃⁻ > SO₄²⁻ > Cl⁻, respectively, in the triangular piper diagram.

Durov plot

An extended Durov plot presented a similar pattern as piper triangular diagram as the greatest percentage of the groundwater samples was classified as “Na + K type” and “Cl type” for cations and anions, respectively (Fig. 7B). The central square depicted a mixture of “Na-Cl type” and “Mixed Ca–Mg–Cl type” for the hydrochemistry of the studied samples. Moreover, pH illustrated a dominant neutral to alkaline water (7.00 to 8.5) containing a TDS range from 0 to 8000 mg L⁻¹. Zidi et al. (2020) reported that Durov diagram displays geochemical processes affecting the water genesis and represents the same classification as piper triangular plot. In our study, Durov plot confirmed the hydrochemistry type of groundwater analyzed by Piper triangular diagram.

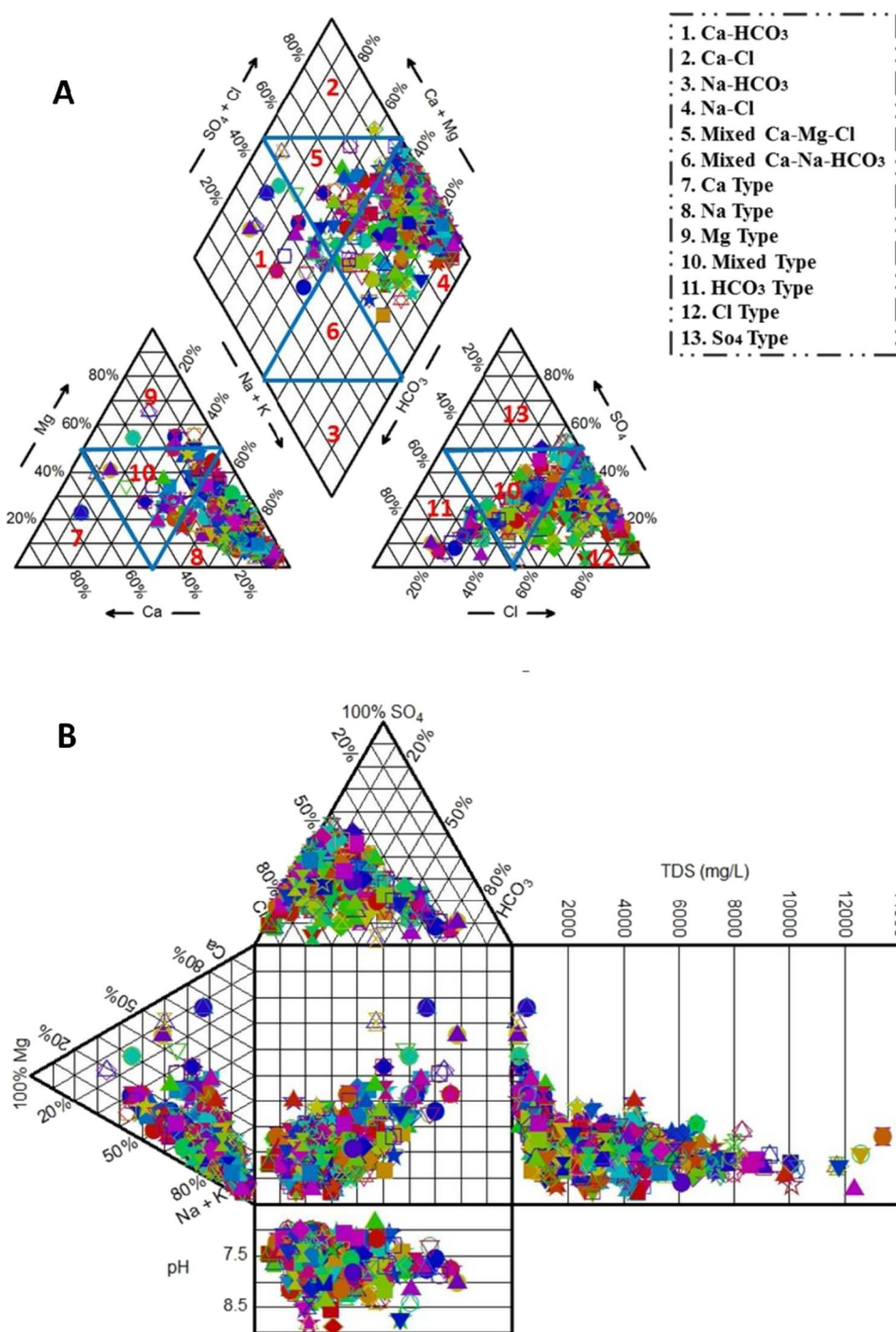
Ficklin-Caboi diagram

The relationships between pH values and metal loads are presented as Ficklin-Caboi plot (Fig. 8A). It is apparent that approximately all the groundwater samples were classified as “near-neutral low metal.” For this, metals in groundwater of the study area were known as low class and less mobile in the aqueous phase. In the water samples, only two samples showed the classification of “near-neutral high metal.” This method firstly introduced by Ficklin and later modified by Caboi to differentiate various characteristics of water chemistry (Laniyan and Adewumi 2021). Based on our findings, all the collected groundwater samples were in “near-neutral low metal” meaning that metals present in the groundwater of the study area classified as “low class” in the aquatic phase. The results indicated that the hydrogeochemical characteristics of the study area have been affected by mining activities as similar conclusions outlined by Zhang et al. (2021).

Schoeller diagram

The major ions contributed in the classification of groundwater samples are demonstrated in Fig. 8B. In the Schoeller diagram, water samples are divided into six groups, including good, acceptable, average, inappropriate, generally unpleasant, and non-drinkable based on their ion contents (Fallahati et al. 2020). According to the results, the water quality classified as good

Fig. 7 Piper trilinear diagram classifying major hydrochemical parameters for groundwater samples in the study area (A) and Durov diagram depicting hydrochemical processes in the groundwater involved (B)



for drinking and irrigation consumptions in all studied groundwater samples because no ion concentration (SO₄, HCO₃, Cl, Mg, Ca, and Na + K) exceeded the value of 200 mg L⁻¹, that met the Iranian National Standards for drinking usages. Schoeller diagram is used to show the quality of water merely based on the dominant cations and anions irrespective of the metals and toxicants; indeed, it is highly possible that water quality classifies as good but contains toxic and carcinogenic metals

(Khalili and Asadi 2021). Sutradhar and Mondal (2021) used Schoeller diagram to assess the suitability and water quality for irrigation and drinking purposes in Suri Sadar Sub-division, West Bengal. They showed that 65.22% and 68% of sampled waters were good for irrigation and drinking usages. In our study area, all sampled waters from wells, springs, and qanats were grouped as good for all applications, i.e., drinking, irrigation, and drinking-irrigation.

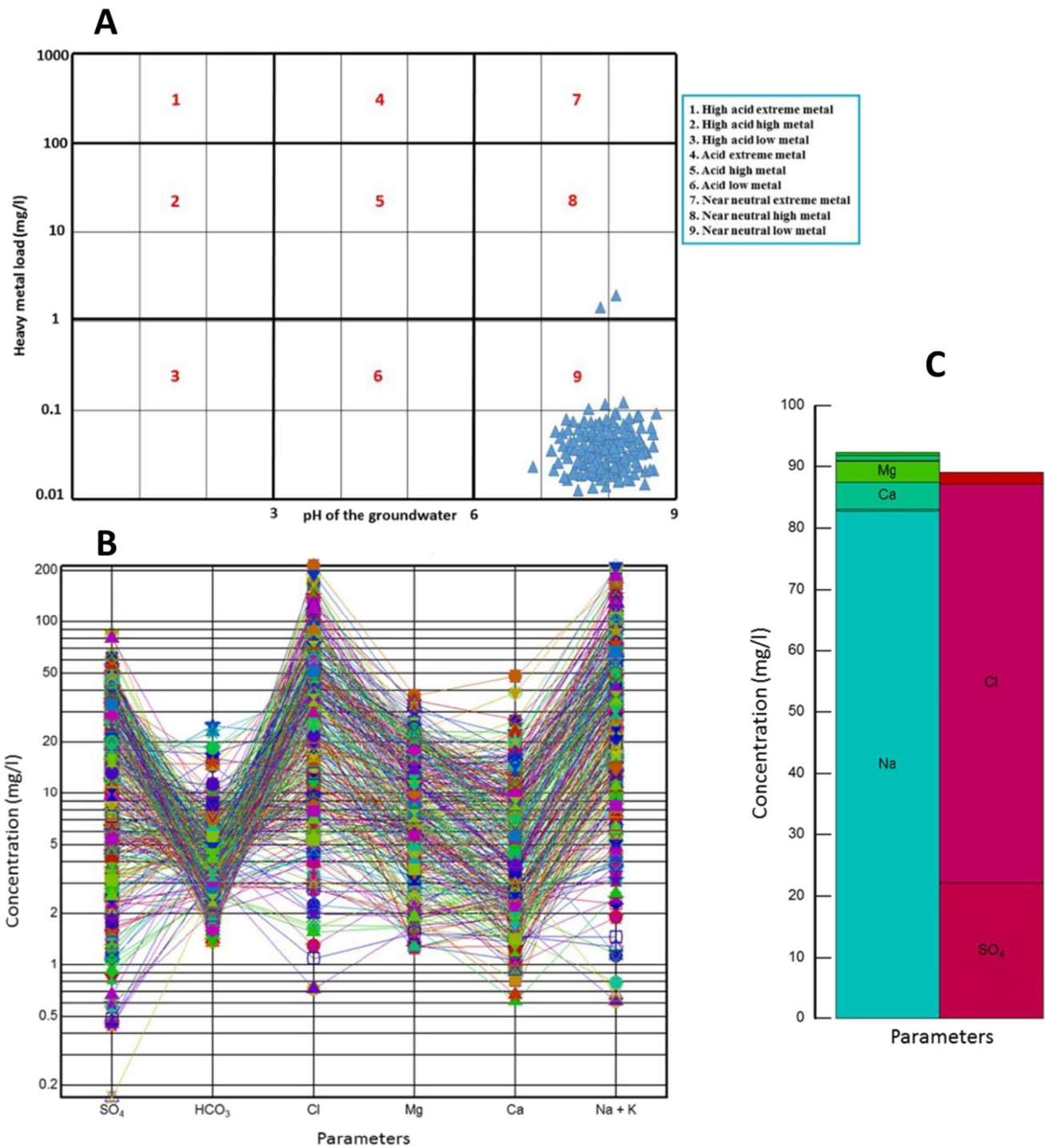


Fig. 8 Ficklin-Caboi diagram classifying the groundwater based on the total heavy metal load and pH of the water samples (A), Schoeller diagram illuminating major ions in the groundwater samples (B), and

ion balance diagram showing the dominant major ions in the groundwater samples (C)

Ion balance diagram

The dominance status of major ions is demonstrated in Fig. 8C. Based on the ion balance diagram, Na and Cl are the most dominant cations and anions, respectively, showing

Na-Cl type of water in the groundwater samples considered. It is apparent that Na^+ , Ca^{2+} , and Mg^{2+} were dominant cations and SO_4^- and Cl^- were prevalent anions in the studied groundwater samples. As shown by piper triangular and Durov plot, Na^+ , Ca^{2+} , Mg^{2+} , SO_4^- , and Cl^- were

considered as the most components of the groundwater samples. Zhang et al. (2012) stated that sodium and salinity could affect the quality of water for drinking and irrigation purposes in exceeding values for dominant cations and anions; however, results emerging to this study revealed no excessive values for salinity and all the sampled locations were suitable for drinking.

Factor analysis

Factor analysis extracted six factors from the water hydrochemical parameters to represent water quality variation in the study area using the rotation technique (Table 9 and Fig. S1). The extracted six factors showed 76.91% of the variation in groundwater quality within the study area. The correlation of the parameters with the factors was significant when it exceeded the radius of the balance circle, which is equal to 0.5 calculated from the square root of the division of the number of factors by the number of the parameters. The first factor/component (factor 1) constituted 38.71% of the trace of the correlation matrix. Factor 1 showed significant correlation with total alkalinity (HCO₃). Component 2 represented 10.80% of the total variance in groundwater quality in the study area and Co, Mo, Sn, Se, and Sb were significantly loaded on this component. These metals did significantly

correlate with each other, but showed a weak correlation with total alkalinity (HCO₃) (Fig. 9). Component 1 suggested a geogenic hydro-geochemical evolution of groundwater by rock-water interaction with ions exchange while component 2 revealed the leaching of materials through rock weathering from soil to the groundwater which are mostly trace elements. Apart from natural sources of Co, Mo, Sn, Se, and Sb, mining activities, agrochemical materials, fertilizers, and municipal waste are responsible for metal pollution of groundwater in South Khorasan (Bodrud-Doza et al., 2020). According to the rotated correlation matrix, EC, total hardness, TDS, SO₄²⁻, Cl⁻, Na⁺, K⁺, Ca²⁺, and Mg²⁺ had significant positive correlations with component 1 at 0.954, 0.938, 0.954, 0.885, 0.921, 0.894, 0.883, and 0.805, respectively (Table 9). In addition, total alkalinity and HCO₃⁻ did significantly correlate with component 2 at 0.984 and 0.986, respectively. In terms of metals, Se (0.858), Sn (0.955), and Sb (0.930) showed highest significant positive correlations with component 3 and 4.

Correlations of trace elements concentration and physiochemical parameters

Spearman’s correlation analysis regarding the potential correlations between studied metals and hydrochemical

Table 9 Rotated component matrix* for hydrochemical parameters and metals measured in different groundwater sources in the study area

Parameter	Component					
	1	2	3	4	5	6
Depth	-0.054	-0.024	-0.116	0.011	0.706	0.349
Water temp	-0.016	-0.148	0.095	0.004	0.795	-0.112
pH	-0.583	-0.162	0.072	0.001	-0.247	-0.177
EC	0.954	-0.081	0.173	-0.011	0.011	-0.103
Salt	-0.032	-0.013	0.018	-0.029	0.089	0.761
Total hardness	0.938	0.026	0.068	0.092	-0.098	0.096
TDS	0.954	-0.081	0.173	-0.011	0.011	-0.103
N-NH ₄ ⁺	0.711	0.112	-0.053	0.104	0.148	0.076
SO ₄ ²⁻	0.885	-0.127	0.173	-0.013	0.000	-0.099
Total alkalinity	-0.074	0.984	0.002	0.017	-0.085	-0.012
HCO ₃ ⁻	-0.070	0.986	0.002	0.017	-0.082	-0.010
Co	0.300	-0.040	0.698	0.190	-0.095	0.261
Se	0.151	0.027	0.858	0.043	-0.082	0.076
Mo	0.041	0.000	0.699	0.022	0.156	-0.307
Sn	0.043	-0.044	-0.002	0.955	0.030	-0.024
Sb	0.037	0.081	0.187	0.930	-0.014	-0.011
Cl ⁻	0.921	-0.154	0.135	-0.022	0.048	-0.122
Na ⁺	0.894	-0.124	0.156	-0.039	0.068	-0.176
K ⁺	0.495	-0.071	0.193	-0.025	-0.266	0.212
Ca ⁺	0.883	-0.119	0.021	0.017	0.016	0.034
Mg ⁺	0.805	0.131	0.089	0.121	-0.169	0.129

*Extraction method, principal component analysis; rotation method, varimax with Kaiser normalization (bold values indicate significant values)

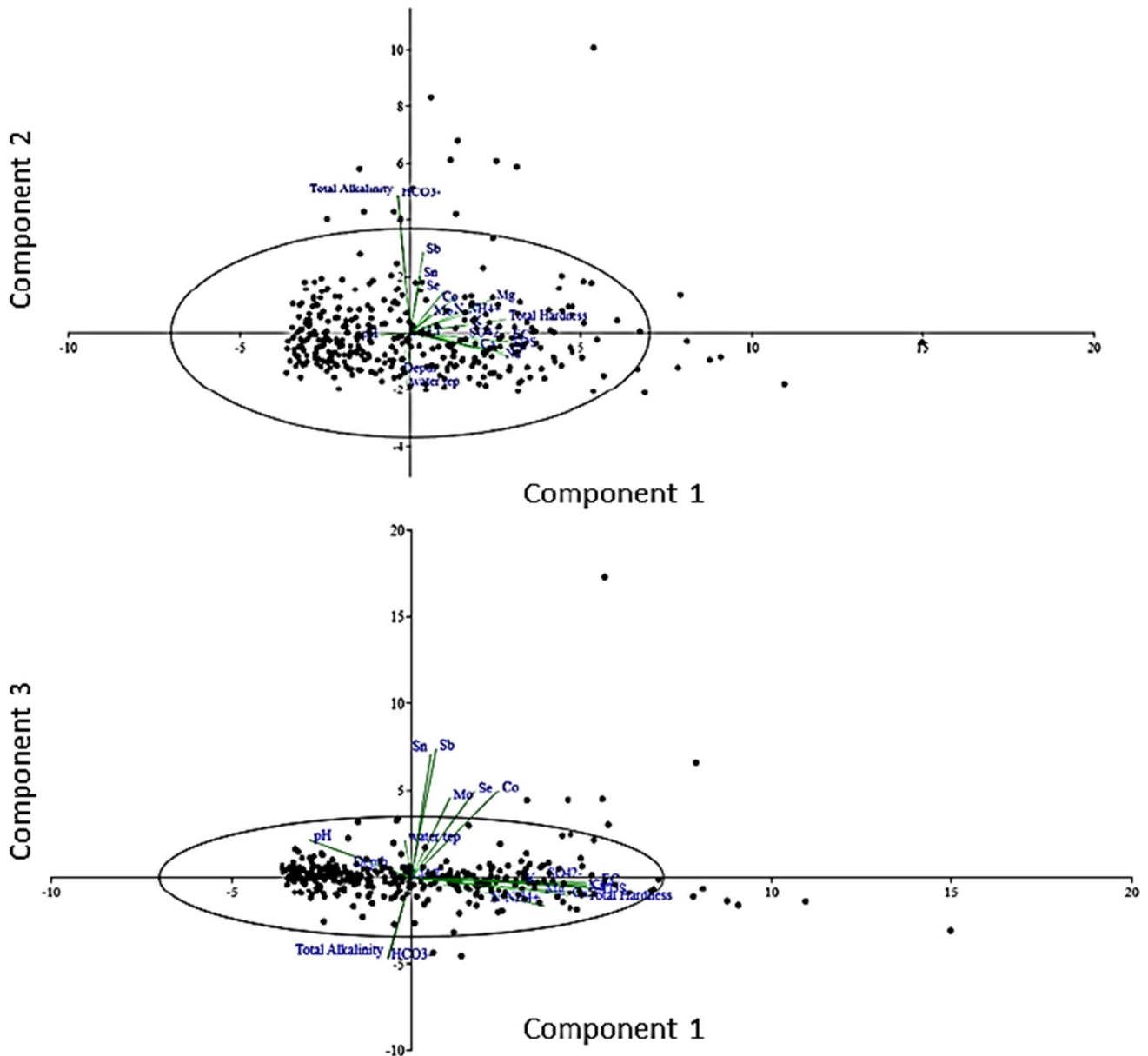


Fig. 9 The weights of component 1 parameters versus components 2 and 3

parameters is portrayed in Table 10. According to the findings, the greatest positive correlations were recorded among EC, TDS, Cl, Na, sulfate, Ca, salt, total hardness, Mg, ammonia, and K^+ measured in the water samples ($Sig < 0.05$). pH presented a correlation with total alkalinity, salt, and ammonia ($Sig < 0.05$). In addition, total alkalinity and bicarbonate and Sn and Sb did significantly correlate in the groundwater of the study area. Parameters such as depth, temperature, total alkalinity, bicarbonate, Sn, and Sb had no significant correlation among the studied hydrochemical parameters ($Sig < 0.05$). Ram et al. (2021) stated that a positive correlation was between alkalinity and ammonia

representing the release of ammonium-based materials into the groundwater. In our study, bicarbonate showed a positive significant correlation with total alkalinity and triggered the alkalinity in the groundwater. In addition, a positive significant correlation was observed between EC and TDS showing the ionic interactions in the groundwater samples. This means that through geochemical reactions various ions are generated in groundwater and therefore TDS consist mainly of ionic constituents that conduct electricity (Atekwana et al. 2004). It is highly possible that in our mining study area, ions originating from mining activities and mineral weathering increase the TDS values and therefore EC.

Table 10 Spearman’s correlation analysis showing the potential relationships among studied hydrochemical parameters

	Depth	Water temp	pH	EC	Salt	Total hardness	TDS	N-NH ₄ ⁺	SO ₄ ²⁻	Alkalinity	HCO ₃ ⁻	Co	Se	Mo	Sn	Sb	Cl ⁻	Na	K	Ca	Mg	
Depth	1.00																					
Water temp	0.30**	1.00																				
pH	-0.03	-0.02	1.00																			
EC	-0.06	-0.09	-0.53**	1.00																		
Salt	-0.051	-0.00	-0.53**	0.98**	1.00																	
Total hardness	-0.04	-0.11*	-0.59**	0.87**	0.86**	1.00																
TDS	-0.06	-0.00	-0.53**	1.00**	0.98**	0.87**	1.00															
N-NH ₄ ⁺	-0.11*	-0.13**	-0.53**	0.80**	0.79**	0.88**	0.80**	1.00														
SO ₄ ²⁻	-0.09	-0.01	-0.54**	0.94**	0.93**	0.84**	0.94**	0.76**	1.00													
Alkalinity	-0.09	-0.25**	0.07	-0.21**	-0.20**	-0.17**	-0.22**	0.03	-0.23**	1.00												
HCO ₃ ⁻	-0.09	-0.25**	0.06	-0.20**	-0.19**	-0.16**	-0.20**	0.01	-0.22**	1.00**	1.00											
Co	-0.09	-0.09	-0.42**	0.62**	0.62**	0.69**	0.62**	0.62**	0.61**	-0.23**	-0.21**	1.00										
Se	-0.15**	-0.01	-0.15**	0.36**	0.35**	0.37**	0.36**	0.35**	0.34**	0.01	0.01	0.56**	1.00									
Mo	-0.09	0.05	0.01	0.26**	0.253**	0.16**	0.26**	0.11*	0.24**	-0.06	-0.06	0.27**	0.36**	1.00								
Sn	-0.05	-0.04	-0.08	0.13**	0.140**	0.15**	0.13**	0.13*	0.16**	-0.04	-0.04	0.24**	0.04	-0.02	1.00							
Sb	-0.16**	-0.10*	-0.05	0.12*	0.127*	0.19**	0.12*	0.15**	0.14**	0.01	0.01	0.34**	0.34**	0.07	0.64**	1.00						
Cl ⁻	-0.02	0.02	-0.48**	0.98**	0.965**	0.83**	0.98**	0.75**	0.90**	-0.27**	-0.27**	0.59**	0.34**	0.26**	0.10	0.08	1.00					
Na	-0.06	0.03	-0.47**	0.97**	0.964**	0.78**	0.97**	0.73**	0.92**	-0.21**	-0.20**	0.56**	0.34**	0.27**	0.11*	0.08	0.98**	1.00				
K	-0.09	-0.10*	-0.37**	0.71**	0.694**	0.70**	0.71**	0.62**	0.66**	-0.15*	-0.10	0.50**	0.31**	0.224**	0.13*	0.19**	0.68**	0.65**	1.00			
Ca	0.01	-0.00	-0.60**	0.83**	0.824**	0.87**	0.83**	0.75**	0.79**	-0.30**	-0.29**	0.63**	0.29**	0.18*	0.06	0.07	0.83**	0.78**	0.63**	1.00		
Mg	-0.07	-0.17**	-0.51**	0.78**	0.774**	0.940**	0.78**	0.84**	0.76**	-0.07	-0.07	0.64**	0.36**	0.17**	0.19**	0.23**	0.73**	0.68**	0.65**	0.67**	1.00	

**Correlation is significant at the 00.01 level (positive: green color; negative: yellow color), * Correlation is significant at the 00.05 level (positive: blue color; negative: purple color), no correlation (red color)

Conclusion

In this mining province, there are more than 670 active mines which significantly impact the soil, environment, and surface and groundwater resources. Qanats, springs, and semi- and deep wells are the most reliable resources in supplying freshwater for people in this province; therefore, the hygiene of such groundwaters directly influences the health of water consumers in this region. For this, the quality and health status of the groundwater in this region play a pivotal role in the health of water consumers. Our results showed that the concentrations of metals ordered as Se > Mo > Sn > Co > Sb and HI did demonstrate a cautious condition for south of South Khorasan (drinking application), southwest of South Khorasan (Irrigation application), and east and center of South Khorasan (drinking-irrigation application). Although trace elements such as Se are essential for

the body function, their exceeding values pose serious hazards to the human health. The type of water, “Na + K type” and “mixed Ca–Mg–Cl type” with an overall group of “Na-Cl-HCO₃” “near-neutral low metal” show that in general groundwater resources classified as “good” for human consumptions. However, the concentration of studied metals and associated non-carcinogenic health risks revealed that there is a concern for the consumers in this heavily mining area. Mining activities in South Khorasan, as the most industrial developments, are accounted for the groundwater contamination, leading to many potential hazards to the human health. In essence, it is strongly recommended that urgent environmental and hygienic programs should be taken into account to mitigate the impacts of mining developments on the groundwater resources in South Khorasan.

Supplementary Information The online version contains supplementary material available at <https://doi.org/10.1007/s11356-022-21494-2>.

Acknowledgements Arvin Zist Pooya Lab is acknowledged for its technical support in the acquisition of the water sample preparation and analysis. The authors also gratefully appreciate Ben Kefford for his revision and helpful guidance in improving this paper.

Author contribution Ali Kazemi: Investigation, supervision, data curation, field sampling. Milad Esmailbeigi: Writing (original draft), data analysis, methodology, graphical analysis. Zahra Sahebi: Conceptualization, funding acquisition, project administration. Sharif Joorabian Shoostari: Review and editing, GIS data management, running GIS data.

Data availability The authors confirm that the data supporting the findings of this study are available within the article.

Declarations

Ethics approval Not applicable.

Consent to participate Not applicable.

Consent to publish Not applicable.

Competing interests The authors declare no competing interests.

References

- Abraham MR, Susan TB (2017) Water contamination with heavy metals and trace elements from Kilembe copper mine and tailing sites in Western Uganda; implications for domestic water quality. *Chemosphere* 169:281–287. <https://doi.org/10.1016/j.chemosphere.2016.11.077>
- Alshaebi FY, Yaacob WZW, Samsudin AR, Alsabahi E (2009) Risk assessment at abandoned tin mine in Sungai Lembing, Pahang, Malaysia. *Electron J Geotech Eng* 14 E:1–9
- Amiri V, Bhattacharya P, Nakhaei M (2021) The hydrogeochemical evaluation of groundwater resources and their suitability for agricultural and industrial uses in an arid area of Iran. *Groundw Sustain Dev* 12:100527. <https://doi.org/10.1016/j.gsd.2020.100527>
- APHA (2005) Standard Methods of Water and Wastewater, 21st edn. American Public Health Association, Washington DC, pp 2–61
- APHA (2012) Standard Methods for the Examination of Water and Waste Water, 22nd edn. American Public Health Association, American Water Works Association, Water Environment Federation
- Arefian FF, Hossein S, Moeini I (2020) Urban heritage along the silk roads. *Springer*. 2365–7588 (1). <https://doi.org/10.1007/978-3-030-22762-3>
- Arya S, Subramani T, Karunanidhi D (2020) Delineation of groundwater potential zones and recommendation of artificial recharge structures for augmentation of groundwater resources in Vattamalaikarai Basin. *South India Environ Earth Sci*. <https://doi.org/10.1007/s12665-020-8832-9>
- Asadi H, Soffianian A, Hemami MR et al (2022) A hybrid GIS-OWA and DANP method for the identification and evaluation of ecotourism attractions: the case study of Abbas Abad Wildlife Refuge, Iran. *GeoJournal*. <https://doi.org/10.1007/s10708-021-10564-6>
- Atekwana EA, Atekwana EA, Rowe RS et al (2004) The relationship of total dissolved solids measurements to bulk electrical conductivity in an aquifer contaminated with hydrocarbon. *J Appl Geophys* 56:281–294. <https://doi.org/10.1016/j.jappgeo.2004.08.003>
- Awadh SM, Al-Mimar H, Yaseen ZM (2021) Groundwater availability and water demand sustainability over the upper mega aquifers of Arabian Peninsula and west region of Iraq. *Environ Dev Sustain*. <https://doi.org/10.1007/s10668-019-00578-z>
- Bakhshi A, Cecchini L, Ghanian M et al (2019) Sustainable irrigation management and farmers' knowledge in South Khorasan. *Iran Int J Sustain Soc* 11:318–335. <https://doi.org/10.1504/IJSSOC.2019.104567>
- Banan A, Forouharmehr A, Reza M, Esmailbeigi M, Bahmani M, Yazdani M, Kolok AS, Rogan EG (2022) Salinity gradients exacerbate the genotoxicity and bioaccumulation of silver nanoparticles in fingerling Persian sturgeon (*Acipenser persicus*). *Reg Stud Mar Sci* 52:102264. <https://doi.org/10.1016/j.rsma.2022.102264>
- Behzadi Tayemeh M, Esmailbeigi M, Shirdel I, Joo HS, Johari SA, Banan A, Nourani H, Mashhadi H, Jami MJ, Tabarrok M (2020) Perturbation of fatty acid composition, pigments, and growth indices of *Chlorella vulgaris* in response to silver ions and nanoparticles: a new holistic understanding of hidden ecotoxicological aspect of pollutants. *Chemosphere* 238:124576. <https://doi.org/10.1016/j.chemosphere.2019.124576>
- Bindal S, Singh CK (2019) Predicting groundwater arsenic contamination: Regions at risk in highest populated state of India. *Water Res* 159:65–76. <https://doi.org/10.1016/j.watres.2019.04.054>
- Bodrud-Doza ISMD, Rume T, Quraishi SB et al (2020) Groundwater for Sustainable Development Groundwater quality and human health risk assessment for safe and sustainable water supply of Dhaka City dwellers in Bangladesh. *Groundw Sustain Dev* 10:100374. <https://doi.org/10.1016/j.gsd.2020.100374>
- Bogard MJ, St-Gelais NF, Vachon D, del Giorgio PA (2020) Patterns of Spring/Summer Open-Water Metabolism Across Boreal Lakes. *Ecosystems* 23:1581–1597. <https://doi.org/10.1007/s10021-020-00487-7>
- Bozorgi M, Moein M, Nejadkoorki F, Toosi NB (2020) Assessing the effect of water scarcity on crop selection and spatial pattern of croplands in central Iran. *Comput Electron Agric* 178:105743. <https://doi.org/10.1016/j.compag.2020.105743>
- Caboi R, Cidu R, Fanfani L, Lattanzi P, Zuddas P (1999) Environmental mineralogy and geochemistry of the abandoned Pb–Zn Montevocchio–Ingurtosu mining district, Sardinia, Italy. *Chron Rech Miniere* 534:21–28
- Cannas D, Loi E, Serra M et al (2020) Relevance of essential trace elements in nutrition and drinking water for human health and autoimmune disease risk. *Nutrients* 12:1–22. <https://doi.org/10.3390/nu12072074>
- Çiner F, Sunkari ED, Şenbaş BA (2021) Geochemical and multivariate statistical evaluation of trace elements in groundwater of Niğde Municipality, South-Central Turkey: implications for arsenic contamination and human health risks assessment. *Arch Environ Contam Toxicol* 80:164–182. <https://doi.org/10.1007/s00244-020-00759-2>
- Colombani N, Gervasio MP, Castaldelli G, Mastrociccio M (2020) Soil conditioners effects on hydraulic properties, leaching processes and denitrification on a silty-clay soil. *Sci Total Environ* 733:139342. <https://doi.org/10.1016/j.scitotenv.2020.139342>
- Cui T, Sreekanth J, Pickett T, Rassam D, Gilfedder M, Barrett D (2021) Impact of model parameterization on predictive uncertainty of regional groundwater models in the context of environmental impact assessment. *Environ Impact Assess Rev* 90:106620. <https://doi.org/10.1016/j.eiar.2021.106620>
- Dawoudian J, Bahamin S, Tantoh HB (2021) Environmental impact assessment of cement industries using mathematical matrix method: case of Ghayen cement, South Khorasan. *Iran Environ Sci Pollut Res* 28:22348–22358. <https://doi.org/10.1007/s11356-020-12012-3>
- dos Luís AA, Cabral P (2021) Small dams/reservoirs site location analysis in a semi-arid region of Mozambique. *Int Soil Water Conserv Res* 9:381–393. <https://doi.org/10.1016/j.iswcr.2021.02.002>

- Egbueri JC (2020) Heavy metals pollution source identification and probabilistic health risk assessment of shallow groundwater in Onitsha, Nigeria. *Anal Lett* 53:1620–1638. <https://doi.org/10.1080/00032719.2020.1712606>
- Eman K, Meško G (2020) Access to safe and affordable drinking water as a fundamental human right: the case of the Republic of Slovenia. *Emerald Handb Crime, Justice Sustain Dev* 1:465–484. <https://doi.org/10.1108/978-1-78769-355-520201025>
- Environmental Protection Agency (EPA) (2004) Risk assessment guidance for superfund volume I human health evaluation manual (Part A). EPA/540/1-89/002
- Esmailbeigi M, Kalbassi MR, Seyedi J, Tayemeh MB, Moghaddam JA (2021) Intra and extracellular effects of benzo [α] pyrene on liver, gill and blood of Caspian White fish (*Rutilus friszi kutum*): Cyto-genotoxicity and histopathology approach. *Mar Pollut Bull* 163:111942. <https://doi.org/10.1016/j.marpolbul.2020.111942>
- Esmailbeigi M, Behzadi Tayemeh M, Johari SA, Ghorbani F, Sourinejad I, Yu IJ (2022) In silico modeling of the antagonistic effect of mercuric chloride and silver nanoparticles on the mortality rate of zebrafish (*Danio rerio*) based on response surface methodology. *Environ Sci Pollut Res*. <https://doi.org/10.1007/s11356-022-19693-y>
- Fallahati A, Soleimani H, Alimohammadi M et al (2020) Impacts of drought phenomenon on the chemical quality of groundwater resources in the central part of Iran—application of GIS technique. *Environ Monit Assess*. <https://doi.org/10.1007/s10661-019-8037-4>
- FAO (1985) Water Quality for Agriculture. Food and Agriculture Organization, Rome
- Ficklin WH, Plumlee GS, Smith KS, McHugh JB (1992) Geochemical classification of mine drainage and natural drainage in mineralized areas. In: Kharaka YK, Maet AS (eds) *Water-rock interaction* 7:81–384
- Ghorbani A, Mousazadeh H, Taheri F et al (2021) An attempt to develop ecotourism in an unknown area: the case of Nehbandan County, South Khorasan Province, Iran. *Environ Dev Sustain* 23:11792–11817. <https://doi.org/10.1007/s10668-020-01142-w>
- Hein C, Van Schaik H, Six D, Mager T, Kolen J, Ertsen M, Nijhuis S, Verschuure-Stuip G (2020) Introduction: Connecting Water and Heritage for the Future. *Adaptive Strategies for Water Heritage*. Springer, Cham. https://doi.org/10.1007/978-3-030-00268-8_1
- Ilieva D, Surleva AR, Murariu M (2018) Evaluation of ICP-OES Method for heavy metal and metalloids determination in sterile dump material. <https://doi.org/10.4028/www.scientific.net/SSP.273.159>
- Iran National Standard Organization (1997) Standards for drinking water in Iran
- Jha MK, Shekhar A, Jenifer MA (2020) Assessing groundwater quality for drinking water supply using hybrid fuzzy-GIS-based water quality index. *Water Res* 179:115867
- Kadam A, Wagh V, Jacobs J et al (2021) Integrated approach for the evaluation of groundwater quality through hydro geochemistry and human health risk from Shivganga river basin, Pune, Maharashtra, India. *Environ Sci Pollut Res*. <https://doi.org/10.1007/s11356-021-15554-2>
- Kazemi A, Riyahi Bakhtiari A, Kheirabadi N, Barani H, Haidari B (2012) Distribution patterns of metals contamination in sediments based on type regional development on the intertidal coastal zones of the Persian Gulf. *Iran Bull Env Contam Toxicol* 88:100–103. <https://doi.org/10.1007/s00128-011-0412-y>
- Kazemi A, Esmailbeigi M, Ansari A, Asl AG, Mohammadzadeh B (2022a) Alterations and health risk assessment of the environmental concentration of heavy metals in the edible tissue of marine fish (*Thunnus tonggol*) consumed by different cooking methods. *Reg Stud Mar Sci* 53:102361. <https://doi.org/10.1016/j.risma.2022.102361>
- Kazemi A, Esmailbeigi M, Sahebi Z, Ansari A (2022b) Health risk assessment of total chromium in the qanat as historical drinking water supplying system. *Sci Total Environ* 807:150795. <https://doi.org/10.1016/j.scitotenv.2021.150795>
- Khalid S, Shahid M, Natasha, et al (2020) Heavy metal contamination and exposure risk assessment via drinking groundwater in Vehari, Pakistan. *Environ Sci Pollut Res* 27:39852–39864. <https://doi.org/10.1007/s11356-020-10106-6>
- Khalili Z, Asadi N (2021) Groundwater quality assessment using Aq.QA and GIS technique in Azna city, Lorestan province, Iran. *Sustain Water Resour Manag* 7:1–12. <https://doi.org/10.1007/s40899-021-00495-y>
- Khan SA, Muhammad S, Nazir S, Shah FA (2020) Heavy metals bounded to particulate matter in the residential and industrial sites of Islamabad, Pakistan: Implications for non-cancer and cancer risks: Evaluation of heavy metals bounded to particulate matter for non-cancer and cancer risks. *Environ Technol Innov* 19:100822. <https://doi.org/10.1016/j.eti.2020.100822>
- Krogulec E, Małeckii JJ, Porowska D, Wojdalska A (2020) Assessment of causes and effects of groundwater level change in an urban area (Warsaw, Poland). *Water* 12(11):3107. <https://doi.org/10.3390/w12113107>
- Kuiper N, Rowell C, Shomar B (2015) High levels of molybdenum in Qatar's groundwater and potential impacts. *J Geochemical Explor* 150:16–24. <https://doi.org/10.1016/j.gexplo.2014.12.009>
- Kumar V, Sharma A, Kumar R et al (2020) Assessment of heavy-metal pollution in three different Indian water bodies by combination of multivariate analysis and water pollution indices. *Hum Ecol Risk Assess* 26:1–16. <https://doi.org/10.1080/10807039.2018.1497946>
- Laniyan TA, Adewumi AJ (2021) Ecological and human health risk associated with potentially toxic metals in water from Ijero mining area, Southwest Nigeria. *Int J Environ Anal Chem* 00:1–25. <https://doi.org/10.1080/03067319.2021.1931159>
- Liu Y, Ma R (2020) Human health risk assessment of heavy metals in groundwater in the luan river catchment within the North China Plain. *Geofluids*. <https://doi.org/10.1155/2020/8391793>
- Long X, Liu F, Zhou X et al (2021) Estimation of spatial distribution and health risk by arsenic and heavy metals in shallow groundwater around Dongting Lake plain using GIS mapping. *Chemosphere* 269:128698. <https://doi.org/10.1016/j.chemosphere.2020.128698>
- Malmal K, Shiri N (2021) Investigating the Importance of Water in Iran Using Game Theory. *J Eng Ind Res* 2:28–35
- Mastrociccio M, Gervasio MP, Busico G, Colombani N (2021) Natural and anthropogenic factors driving groundwater resources salinization for agriculture use in the Campania plains (Southern Italy). *Sci Total Environ* 758:144033. <https://doi.org/10.1016/j.scitotenv.2020.144033>
- Michel S, Ghoddousi A (2020) *Ovis vignei*. The IUCN Red List of Threatened Species 2020: e.T54940655A54940728. <https://doi.org/10.2305/IUCN.UK.2020.2.RLTS.T54940655A54940728.en>
- Mohamed A (2019) Hydro-geophysical study of the groundwater storage variations over the Libyan area and its connection to the Dakhla basin in Egypt. *J African Earth Sci* 157:103508. <https://doi.org/10.1016/j.jafrearsci.2019.05.016>
- Mridha MAH, Rahman SH (2021) Prediction of groundwater trends for irrigation in Northern Bangladesh. *Water Supply* 21:2596–2614. <https://doi.org/10.2166/ws.2021.076>
- Nivetha A, Sakthivel C, Prabha I (2021) Heavy metal contamination in groundwater and impact on plant and human. 233–246. https://doi.org/10.1007/978-3-030-63422-3_14
- Njora B, Yilmaz H (2021) Evaluation of water accessibility, distribution, water use policies and management in Kenya. *International Journal of Water Management and Diplomacy* 1:5–16. <https://dergiipark.org.tr/en/pub/ijwmd/issue/63570/958552>

- Noreen F, Sajjad A, Mahmood K et al (2020) Human biomonitoring of trace elements in scalp hair from healthy population of Pakistan. *Biol Trace Elem Res* 196:37–46. <https://doi.org/10.1007/s12011-019-01906-0>
- O'Driscoll M (2008) Magnesite ignites. *Ind Miner* 28–45
- Obasi PN, Akudinobi BB (2020) Potential health risk and levels of heavy metals in water resources of lead–zinc mining communities of Abakaliki, southeast Nigeria. *Appl Water Sci*. <https://doi.org/10.1007/s13201-020-01233-z>
- Parang H, Esmailbeigi M (2022) Total mercury concentration in the muscle of four mostly consumed fish and associated human health risks for fishermen and non-fishermen families in the Anzali Wetland, Southern Caspian Sea. *Reg Stud Mar Sci* 52:102270. <https://doi.org/10.1016/j.rsma.2022.102270>
- Peng K, Li X, Wang Z (2015) Hydrochemical characteristics of groundwater movement and evolution in the Xinli deposit of the Sanshandao gold mine using FCM and PCA methods. *Environ Earth Sci*. <https://doi.org/10.1007/s12665-014-3938-6>
- Phan VH, Dinh VT, Su Z (2020) Trends in long-term drought changes in the Mekong River Delta of Vietnam. *Remote Sens* 12(18):1–22. <https://doi.org/10.3390/RS12182974>
- Piesse M (2020) Global water supply and demand trends point towards rising water insecurity. *Future Directions International* 27(7):2020. <https://apo.org.au/node/276976>
- Qiao J, Zhu Y, Jia X et al (2020) Distributions of arsenic and other heavy metals, and health risk assessments for groundwater in the Guanzhong Plain region of China. *Environ Res* 181:108957. <https://doi.org/10.1016/j.envres.2019.108957>
- Rajasekhar B, Nambi IM, Govindarajan SK (2020) Human health risk assessment for exposure to BTEXN in an urban aquifer using deterministic and probabilistic methods: a case study of Chennai city. *India Environ Pollut* 265:114814. <https://doi.org/10.1016/j.envpol.2020.114814>
- Rajmohan N, Masoud MHZ, Niyazi BAM (2021) Impact of evaporation on groundwater salinity in the arid coastal aquifer. *Western Saudi Arabia Catena* 196:104864. <https://doi.org/10.1016/j.catena.2020.104864>
- Ram A, Pandey SKTHK, Kumar A et al (2021) Groundwater quality assessment using water quality index (WQI) under GIS framework. *Appl Water Sci* 11:1–20. <https://doi.org/10.1007/s13201-021-01376-7>
- Ravanipour M, Hadi M, Rastkari N et al (2021) Presence of heavy metals in drinking water resources of Iran: a systematic review and meta-analysis. *Environ Sci Pollut Res* 28:26223–26251. <https://doi.org/10.1007/s11356-021-13293-y>
- Ravikumar P, Somashekar R, Prakash K (2015) A comparative study on usage of Durov and Piper diagrams to interpret hydrochemical processes in groundwater from SRLIS river basin, Karnataka, India. *Earth Sci* 80:31073–31077
- Saxena VK, Singh VS, Mondal NC, Jain SC (2003) Use of hydrochemical parameters for the identification of fresh groundwater resources, Potharlanka Island, India. *Environ Geol* 44:516–521. <https://doi.org/10.1007/s00254-003-0807-0>
- Sayadi MH, Kharkan J, Binkowski LJ et al (2020) Cadmium and chromium levels in water and edible herbs in a risk assessment study of rural residents living in Eastern Iran. *Environ Sci Pollut Res* 27:9901–9909. <https://doi.org/10.1007/s11356-020-07600-2>
- Seyedi J, Kalbassi MR, Esmailbeigi M, Tayemeh MB, Amiri Moghadam J (2021a) Toxicity and deleterious impacts of selenium nanoparticles at supranutritional and imbalance levels on male goldfish (*Carassius auratus*) sperm. *J Trace Elem Med Biol* 66:126758. <https://doi.org/10.1016/j.jtemb.2021.126758>
- Seyedi J, Tayemeh MB, Esmailbeigi M, Joo HS, Langeroudi EK, Banan A, Johari SA, Jami MJ (2021b) Fatty acid alteration in liver, brain, muscle, and oocyte of zebrafish (*Danio rerio*) exposed to silver nanoparticles and mitigating influence of quercetin-supplemented diet. *Environ Res* 194:110611. <https://doi.org/10.1016/j.envres.2020.110611>
- Shams M, Tavakkoli Nezhad N, Dehghan A et al (2020) Heavy metals exposure, carcinogenic and non-carcinogenic human health risks assessment of groundwater around mines in Joghatai, Iran. *Int J Environ Anal Chem* 00:1–16. <https://doi.org/10.1080/03067319.2020.1743835>
- Shirazi A, Shirazy A, Karami J (2018) Remote sensing to identify copper alterations and promising regions, Sarbishe, South Khorasan, Iran. *Int J Geol Earth Sci* 4:36–52
- Shirdel I, Kalbassi MR, Esmailbeigi M, Tinoush B (2020) Disruptive effects of nonylphenol on reproductive hormones, antioxidant enzymes, and histology of liver, kidney and gonads in Caspian trout smolts. *Comp Biochem Physiol Part C Toxicol Pharmacol* 232:108756. <https://doi.org/10.1016/j.cbpc.2020.108756>
- Siebert S (2021) Water use in human civilizations: an interdisciplinary analysis of a perpetual social-ecological challenge. *Front Agric Sci Eng*. <https://doi.org/10.15302/j-fase-2021393>
- Soleimani H, Azhdarpoor A, Hashemi H et al (2020) Probabilistic and deterministic approaches to estimation of non-carcinogenic human health risk due to heavy metals in groundwater resources of torbat heydariyeh, southeastern of Iran. *Int J Environ Anal Chem* 1:1–15. <https://doi.org/10.1080/03067319.2020.1757086>
- Søndergaard J, Asmund G, Larsen MM (2015) Trace elements determination in seawater by ICP-MS with on-line pre-concentration on a Chelex-100 column using a “standard” instrument setup. *MethodsX* 2:323–330. <https://doi.org/10.1016/j.mex.2015.06.003>
- Sutradhar S, Mondal P (2021) Groundwater suitability assessment based on water quality index and hydrochemical characterization of Suri Sadar Sub-division, West Bengal. *Ecol Inform* 64:101335. <https://doi.org/10.1016/j.ecoinf.2021.101335>
- Talebi MS, Fatemi M (2020) Assessment of the quality and quantity of groundwater in Bahadoran plain using neural network methods, geostatistical and multivariate statistical analysis. *J Appl Res Water Wastewater* 14(14):144–151
- Tiwari AK, De Maio M (2017) Assessment of risk to human health due to intake of chromium in the groundwater of the Aosta Valley region, Italy. *Hum Ecol Risk Assess* 23:1153–1163. <https://doi.org/10.1080/10807039.2017.1308813>
- Tsai KS, Chang YM, Kao JCM, Lin KL (2016) Groundwater molybdenum from emerging industries in Taiwan. *Bull Environ Contam Toxicol* 96:102–106. <https://doi.org/10.1007/s00128-015-1695-1>
- Umamageswari TSR, Sarala Thambavani D, Liviu M (2019) Hydrogeochemical processes in the groundwater environment of Batlagundu block, Dindigul district, Tamil Nadu: conventional graphical and multivariate statistical approach. *Appl Water Sci* 9:1–15. <https://doi.org/10.1007/s13201-018-0890-8>
- United States Environmental Protection Agency (US EPA) (2012) Standard Operating Procedure for an In Vitro Bioaccessibility Assay for Lead in Soil. EPA 9200.2–86.
- USEPA (2004) Overview of the ecological risk assessment process in the office of pesticide programs, US Environmental Protection Agency. Office of Prevention, Pesticides and Toxic Substances Office of pesticides Programs. Washington, DC, p 92
- Vasilache N, Vasile GG, Diaconu E et al (2020) Groundwater quality assessment for drinking and irrigation purpose using GIS, Piper diagram, and water quality index. *Rom J Ecol Environ Chem* 2:109–117. <https://doi.org/10.21698/rjeec.2020.214>
- Veisi S, Johari SA, Tyler CR, Mansouri B, Esmailbeigi M (2021) Antioxidant properties of dietary supplements of free and nanoencapsulated silymarin and their ameliorative effects on silver nanoparticles induced oxidative stress in Nile tilapia (*Oreochromis niloticus*). *Environ Sci Pollut Res* 28:26055–26063. <https://doi.org/10.1007/s11356-021-12568-8>

- Wang X, Cui L, Li J et al (2021a) Ecological and health risk assessments and water quality criteria of heavy metals in the Haihe River. *Environ Pollut*. <https://doi.org/10.1016/j.envpol.2021.117971>
- Wang H, Yang Q, Ma H, Liang J (2021b) Chemical compositions evolution of groundwater and its pollution characterization due to agricultural activities in Yinchuan Plain, northwest China. *Environ Res* 200:111449. <https://doi.org/10.1016/j.envres.2021.111449>
- WHO (2011) Nitrate and Nitrite in Drinking Water (WHO/SDE/WSH/07.01/16/Rev/1). Background document for development of WHO guidelines for drinking water quality, Geneva, Switzerland
- Wu C, Fang C, Wu X, Zhu G (2020) Health-risk assessment of arsenic and groundwater quality classification using random forest in the Yanchi Region of Northwest China. *Expo Heal* 12:761–774. <https://doi.org/10.1007/s12403-019-00335-7>
- Yakameran E, Ari A, Aygün A (2021) Land application of municipal sewage sludge: human health risk assessment of heavy metals. *J Clean Prod* 319:128568. <https://doi.org/10.1016/j.jclepro.2021.128568>
- Zakir HM, Sharmin S, Akter A, Rahman MS (2020) Assessment of health risk of heavy metals and water quality indices for irrigation and drinking suitability of waters: a case study of Jamalpur Sadar area, Bangladesh. *Environ Adv* 2:100005. <https://doi.org/10.1016/j.envadv.2020.100005>
- Zhang C, Duan Q, Yeh PJ, Pan Y, Gong H (2021) Sub-regional groundwater storage recovery in North China Plain after the South-to-North water diversion project. *J Hydrol* 597:126156. <https://doi.org/10.1016/j.jhydrol.2021.126156>
- Zhang N, Suleiman JS, He M, Hu B (2008) Chromium(III)-imprinted silica gel for speciation analysis of chromium in environmental water samples with ICP-MS detection. *Talanta* 75:536–543. <https://doi.org/10.1016/j.talanta.2007.11.059>
- Zhang Y, Li F, Ouyang Z (2012) Distribution and health risk assessment of heavy metals of groundwaters in the irrigation district of the lower reaches of Yellow River. *Environ Sci* 34(1):121–130
- Zidi C, Jamrah A, Al-Issai L (2020) Hydrochemical assessment of groundwater, case study Al-Zaroub aquifer, Buraimi Governorate, Sultanate of Oman. *Groundw Sustain Dev* 11:100450. <https://doi.org/10.1016/j.gsd.2020.100450>
- Zubaidi SL, Ortega-Martorell S, Al-Bugharbee H et al (2020) Urban water demand prediction for a city that suffers from climate change and population growth: Gauteng province case study. *Water (switzerland)* 12:1–17. <https://doi.org/10.3390/W12071885>
- Zuo TT, Jin HY, Zhang L et al (2020) Innovative health risk assessment of heavy metals in Chinese herbal medicines based on extensive data. *Pharmacol Res* 159:104987. <https://doi.org/10.1016/j.phrs.2020.104987>

Publisher's note Springer Nature remains neutral with regard to jurisdictional claims in published maps and institutional affiliations.